

1 Interferon gamma prevents infectious entry of HPV16 via an L2-dependent mechanism

2

3 Patricia M. Day[#], Cynthia D. Thompson, Douglas R. Lowy, John T. Schiller

4

5 Laboratory of Cellular Oncology, NCI, NIH, Bethesda, MD 20892 USA

6 [#] corresponding author: pmd@nih.gov

7

8

9 running title: IFN- γ inhibits HPV16 infection

10

11 Abstract word count: 170

12 Text word count: 7435

13

14 Key words: HPV, papillomavirus, interferon, IFN-gamma, L2

15

16 **Abstract:** In this study, we report that IFN- γ , but not IFN α , β or λ treatment, dramatically
17 decreased infection of HPV16 pseudovirus (PsV). In a survey of 20 additional HPV and animal
18 papillomavirus type, we found that many, but not all, PsV types were also inhibited by IFN- γ .
19 Microscopic and biochemical analyses of HPV16 PsV determined that the antiviral effect was exerted at
20 the level of endosomal processing of the incoming capsid and depended on the JAK2/STAT1 pathway. In
21 contrast to infection in the absence of IFN- γ , where L1 proteolytic products are produced during
22 endosomal capsid processing and L2/DNA complexes segregate from L1 in the late endosome and travel
23 to the nucleus, IFN- γ treatment led to decreased L1 proteolysis and retention of L2 and the viral genome
24 in the late endosome/lysosome. PsV sensitivity or resistance to IFN- γ treatment was mapped to the L2
25 protein, as determined with infectious hybrid PsV in which the L1 protein was derived from an IFN- γ -
26 sensitive HPV type and the L2 protein from an IFN- γ -insensitive type, or vice versa.

27
28
29 **Importance:** A subset of human papillomaviruses (HPV) are the causative agents of many
30 human cancers, most notably cervical cancer. This manuscript describes the inhibition of infection of
31 multiple HPV types, including oncogenic types, by treatment with interferon- γ , an antiviral cytokine that
32 is released from stimulated immune cells. Exposure of cells to IFN- γ has been shown to trigger the
33 expression of proteins with broad antiviral effector functions, most of which act to prevent viral
34 transcription or translation. Interestingly, in this study, we show that infection is blocked at the early
35 step of virus entry into the host cell by retention of the minor capsid protein, L2, and the viral genome,
36 instead of trafficking into the nucleus. Thus, a novel antiviral mechanism for interferon- γ has been
37 revealed.

38

39

40 Papillomaviruses (PVs) are members of a large group of non-enveloped DNA tumor viruses that
41 infect epithelial tissues of a wide range of vertebrate species. A subset of oncogenic mucosal human PV
42 (HPV) types are the causal agents of cervical cancer. These “high-risk” types, especially HPV16, are also
43 linked to vulvar, vaginal, anal, and oropharyngeal cancers (1). The cascade of viral protein expression is
44 integrally tied to epithelial differentiation, with virion production only occurring in the terminally
45 differentiated upper layers (2). These features combine to allow circumvention of host innate and
46 adaptive immune responses, as few pro-inflammatory signals are elicited during these early stages (3).
47 However, most PV infections that induce overt hyperproliferation are eventually cleared with the
48 apparent involvement of lymphocytic infiltrates (reviewed in (4)). Also, HPV infections are often
49 superimposed on colonization with other microbial agents, e.g. in the female reproductive tract
50 (reviewed in (5)). It is, therefore, of interest to determine if anti-viral molecules that are known
51 components of the innate or adaptive immune response to other infections could inhibit PV infection.
52 In this regard, there has been a single report of type I interferons inhibiting in vitro HPV16 infection (6).

53 The IFNs are a family of secreted polypeptides that were first identified by their ability to induce
54 cellular resistance to viral infection (7). Type I interferons, including IFN- α and IFN- β , are released from
55 many virally-infected cells, and interact with a shared, broadly expressed plasma membrane receptor (8,
56 9). The more recently described type III IFNs (IFN- λ) are also induced by viral infection (10). However,
57 IFN- λ receptors are largely restricted to cells of epithelial origin, resulting in a narrower cellular response
58 to pathogens (9). The sole type II IFN, IFN- γ , is released from activated T lymphocytes and NK cells (9).
59 IFN- γ is critical for macrophage activation in response to microbial infection, but a wide variety of other
60 cell types, including epithelial cells, express its receptor, IFNGR, and are responsive to IFN- γ activation (8,
61 9). The antiviral activity of IFN- γ can either occur directly through the induction of effector molecules or
62 indirectly through enhanced antigen presentation.

63 One technical consequence of the restriction of the productive PV life cycle to the terminally
64 differentiating epithelium is the resultant difficulty in obtaining authentic viral particles. The
65 pseudovirus (PsV) production system, which is an alternative to authentic virus, has been used most
66 often to examine early events in PV infection, including host cell binding and entry (11-13). These
67 surrogate particles contain the two capsid proteins, the major protein, L1, and the minor protein, L2,
68 and encapsidate a plasmid termed a pseudogenome, which encodes a reporter protein. Expression of
69 this reporter indicates successful completion of the entry process. PV initially interact with heparan
70 sulfate proteoglycans (HSPGs) on either the cell surface (in vitro) or basement membrane (in vivo) (14-
71 16). This interaction induces distinct conformational changes in the capsids, including the critical
72 exposure of the amino terminus of L2, which contains a conserved furin cleavage site that must be
73 proteolytically processed for successful infection (17, 18). Capsid endocytosis proceeds via a novel
74 pathway which is most closely related to macropinocytosis (19). The viral particles traverse the
75 endosomal system via early endosomes and are subsequently delivered to late endosomes
76 (LE)/lysosomes (20, 21). In the presence of lysosomotropic agents, infection is abolished, and the
77 particles accumulate in the LE/lysosomal compartment (19). The majority of the major capsid protein,
78 L1, is retained within this compartment, whereas L2 and the genome are segregated from L1 and
79 delivered into the trans-Golgi network (TGN) via a Rab7b- and Rab9a-dependent manner prior to their
80 delivery to the nucleus (22). Retromer-dependent transport of the L2/DNA complex from the early
81 endosome has also been presented as an alternative mode of entry to the TGN (23, 24). Entry into the
82 nucleus requires mitosis, after which the L2/DNA complex localizes to the subnuclear domain ND10,
83 where transcription of the virally-delivered DNA can occur (25, 26).

84 In this study, we have evaluated the effect of various classes of IFNs on HPV PsV infection in
85 vitro. Although many studies have examined the consequences of various IFNs on overall replication of
86 a range of viruses, very few reports have examined the effects of IFNs on the early stages of the viral life

87 cycle in which the PsV participate. Our study documents potent inhibition of many, but not all, HPV PsV
88 by IFN- γ , but not other IFNs.

89

90 **MATERIALS AND METHODS**

91 **Reagents.** Sources for IFNs are as follows: Recombinant human interferon gamma (ProSpec cyt-206,
92 >98% purity); recombinant mouse interferon gamma (ProSpec cyt-358, >95% purity); recombinant
93 human interferon alpha 2b (ProSpec cyt-205, >98% purity); recombinant human interferon alpha 2a
94 (ProSpec cyt-204, >97% purity); recombinant human interferon lambda 1 (PeproTech 300-02L, >98%
95 purity). Additionally, human leukocyte IFN- α (NR-3078) and human recombinant IFN- β (NR-3085) were
96 obtained through BEI Resources, NIAID, NIH (purity levels not given). The inhibitors PF-573228 (S2013,
97 >99% purity), Ruxolitinib (S1378, >99% purity), U1026 (S1102, >99% purity) and CEP-33779 (S2806,
98 >99% purity) were obtained from Selleck Chemicals. The inhibitors imidazole-oxindole (C16) (I9785,
99 >98% purity) and Stattic (S7947, >98% purity) were obtained from Sigma-Aldrich. Fluorescein-labeled
100 Ricinus Communis Agglutinin II (ricin) (FL-1091) was purchased from Vector laboratories. Cholera Toxin
101 subunit B conjugated to Alexa fluor 488 (C34775) and Alexa fluor 488-conjugated epidermal growth
102 factor (EGF) (E-13345) were purchased from Invitrogen.

103 **Cell lines.** The human keratinocyte cell line, HaCaT, originally from Norbert Fusenig (27), and the HeLa
104 and 293TT (11) cell lines were cultured in DMEM media supplemented with 10% fetal bovine serum
105 (FBS) and penicillin/streptomycin (P/S). The murine keratinocyte cell line, S1, was a kind gift from Stuart
106 Yuspa (NCI, NIH) (28). The epithelial ectocervical cell line, Ect1 E6/E7, was obtained from ATCC (CRL-
107 2614). Both of these cell lines were also cultivated in DMEM with 10% FBS, P/S. SK-MEL-2 and SK-MEL-
108 28 are part of the NCI-60 tumor cell line panel and were obtained from the Developmental Therapeutics
109 Program at the National Cancer Institute, NIH (Frederick, MD).

110 **Antibodies.** The rabbit polyclonal antisera recognizing HPV16 and HPV45 capsids were previously
111 described (29, 30), as were the anti-L2 monoclonal antibodies, K1L2 (L2 amino acids 64-81) used for
112 immunofluorescent detection and K5L2 (56-75) used for Western blot detection, kind gifts from Martin
113 Müller (DKFZ, Heidelberg) (31). The anti-LAMP-1 monoclonal antibody (H4A3) developed by August and
114 Hildreth was obtained from the Developmental Studies Hybridoma Bank developed under the auspices
115 of NICHD and maintained by the Department of Biological Sciences at the University of Iowa (32). All
116 other antibodies were obtained from commercial sources. Camvir-1 antibody (Abcam) was used to
117 detect HPV16 L1 on Western blots. Rabbit anti-giantin was obtained from BioLegend (924302). Mouse
118 anti-TFR was purchased from Zymed (13-6800). Rabbit anti-GAPDH (14C10), rabbit anti ERK1/2 (9102S),
119 rabbit anti pERK1/2 (9101S), rabbit anti-STAT3 (12640S) and rabbit anti-pSTAT3 (9145S) were from Cell
120 Signaling Technology. The antibodies against FAK (610087) and pFAK (611723) were from Becton
121 Dickinson. The antibodies recognizing EGFR (sc-03), STAT1 (sc-346), and tyrosine 701-phosphorylated
122 STAT1 (sc-13648) were all purchased from Santa Cruz Biotechnology, Incorporated.

123 **Pseudovirus production.** PsV preparations were produced according to the improved, standard method
124 production protocol published on the laboratory website (<http://home.ccr.cancer.gov/lco/plasmids.asp>)
125 (33). Briefly, 293TT cells were transfected with either a bicistronic plasmid encoding the PV L1 and L2
126 proteins or two plasmids separately encoding the capsid proteins, together with a reporter gene plasmid
127 encoding GFP (pfbW). Purity and L1 content were assessed following protein staining of SDS-Page gels
128 with SimplyBlue SafeStain, a Coomassie G-250 stain, (Invitrogen). For infection, PsV were used at a
129 concentration titrated to yield 15-30% GFP positivity. The ng amount (based on L1 content) needed to
130 obtain this infectivity varies according to PsV type and is noted after the type. The plasmids used for the
131 various types were: HPV16 (2 ng), p16sheLL; HPV5 (40 ng), p5shell; HPV6 (40 ng), p6sheLL; HPV11 (50
132 ng), p11L1w and p11L2w; HPV18 (2 ng), p18sheLL; HPV31 (10 ng), p31sheLL; HPV45 (1 ng), p45sheLL;
133 HPV52 (65 ng), p52sheLL; HPV58 (4 ng), p58sheLL. For the additional types HPV8 (80 ng), HPV26 (2 ng),

134 HPV33 (3 ng), HPV38 (100 ng), HPV39 (2 ng), HPV40 (40 ng), HPV59 (5 ng), HPV68 (4 ng) and HPV73 915
135 ng), we used the corresponding pVITRO bicistronic expression plasmid described by Kwak et al. (34),
136 kind gifts from Richard Roden (Johns Hopkins University). For assembly of the hybrid PsV particles,
137 HPV45/16 (15 ng), HPV18/45 (3 ng) and HPV45/18 (2 ng) the following plasmids were used: HPV16 L1,
138 p16L1h; HPV16L2, p16L2h, both generated in our laboratory, and HPV45L1, HPV45L1HD; HPV45L2,
139 HPV45L2HD; HPV18L1, HPV18L1HD; HPV18L2, HPV18L2HD, which were all kind gifts from Martin Müller
140 (DKFZ). Where indicated, PsV were assembled in the presence of 50 μ M 5-ethynyl-2'-deoxyuridine
141 (EdU) supplemented to the growth medium at 6 hours post-transfection as previously described (22).
142 Assembled particles were released by detergent lysis, matured in the presence of 25 mM ammonium
143 sulfate and purified by ultracentrifugation through an Optiprep step gradient (33). For control
144 experiments, HPV16 PsV packaging pLucf, which encodes both GFP and firefly luciferase, was produced.
145 Quantification of luciferase activity was performed with the Britelite plus kit (6066761, Perkin Elmer)
146 according to the manufacturer's directions.

147 **Pseudovirus infection.** To assess infection, PsV dilutions were added to HaCaT cells that had been
148 grown overnight at a plating density of 8×10^3 cells per well in 96 well plates. The percent of GFP-
149 transduced cells was determined by flow cytometric analysis (BD FACScaliber) after a 48-72 hour
150 infection period. Prior to analysis, cells were dislodged with 50 μ l 0.25% trypsin. Following this 150 μ l
151 of FACS buffer (PBS containing 2% FBS and 0.1% sodium azide) was added to each well and cells were
152 processed on a Becton Dickinson FACS Canto II cytometer equipped with a high throughput plate reader.
153 Live cells were selectively gated by FSC/SSC considerations. Addition of IFN was performed 18 hours
154 prior to initiation of PsV infection unless otherwise noted. Biochemical inhibitors of potential IFN
155 activation were added immediately prior to IFN addition. All flow cytometry experiments were
156 performed in triplicate and repeated a minimum of three times.

157 **Immunofluorescent staining.** Cells were seeded onto glass No. 01 coverslips in a 24-well plate at a
158 density of 8×10^4 /well and cultured overnight. For evaluation of internalized PsV, 20 ng of PsV were
159 added to each well and allowed to bind and internalize for 24 hours. Following this incubation cells
160 were fixed in ice cold ethanol containing 15 mM glycine and processed for immunofluorescent staining.
161 Detection of EdU-labeled pseudogenomes was performed with the Click-It 488 Alexa Fluor EdU Imaging
162 kit (Invitrogen) as previously described (22). For visualization of other cargo, incubation was performed
163 for time period indicated in the text. EGF-488 was used at a concentration of 1 $\mu\text{g/ml}$, CTXB-488 was
164 used at 5 $\mu\text{g/ml}$, ricin-FITC was used at 10 $\mu\text{g/ml}$. Following these incubations, the cells were fixed in 2%
165 paraformaldehyde in PBS for 20 minutes at room temperature. At which time, the coverslips were
166 washed in PBS containing 200 mM glycine, and processed for immunofluorescent detection of marker
167 proteins as previously described (35). Stained coverslips were mounted by inversion onto DAPI-
168 containing solution (Prolong Gold, Molecular Probes). All images were acquired with a Zeiss 780
169 confocal system interfaced with a Zeiss Axiovert 100M microscope. Images were collated with Adobe
170 Photoshop software. The inserts in Figure 2, panels A and B, show surface-rendered images of Z-stack
171 images that were processed with Imaris software. Lysosomal diameters were measured with the Imaris
172 software following surface rendering. Significance was determined using Welch's unequal variances t-
173 test. The colocalization histograms shown in Figure 2, panels C-F, were created by line profile analysis in
174 the Zen software (Zeiss). The pixel values were exported to GraphPad Prism 7.

175 **PsV processing.** To examine the intracellular processing of HPV16 PsV, 4×10^5 HaCaT cells/well were
176 plated in 6 well plates overnight and then treated with 2 ng/ml IFN- γ prior to incubation with PsV. 900
177 ng of PsV, based on L1 protein amount, was added per well and incubated for the indicated time.
178 Following this cells were removed with 0.25% trypsin, washed twice with PBS and lysed in
179 immunoprecipitation (IP) buffer (50 mM Tris-HCl pH 8.0, 100 mM NaCl, 50 mM NaF, 0.5% NP-40 and
180 0.1% SDS containing Complete protease inhibitor cocktail (Roche)) for 20 minutes on ice. Cellular debris

181 was removed by centrifugation. Clarified lysates were incubated with rabbit anti-HPV16 L1 VLP
182 antiserum and protein A/G sepharose (Pierce) overnight in the cold with rocking. Immunoprecipitated
183 complexes were collected by centrifugation and washed 4 times in IP buffer. The remaining complexes
184 were boiled in SDS-PAGE sample buffer and resolved on a 4-12% NuPage gel (Invitrogen) and transferred
185 to an Immobilon membrane (Millipore). HPV16 L1 was detected with the Camvir1 antibody. For
186 determination of L1-associated L2 protein, the above procedure was followed. If indicated, the addition
187 of NH_4Cl was coincident with the addition of PsV to a final concentration of 20 mM. L2 was detected by
188 Western blot analysis with the K5L2 (56-75) antibody.

189 **EGFR processing.** To evaluate the cellular processing of EGFR, 4×10^5 cells HaCaT cells, plated in 12 well
190 plates were either untreated or IFN- γ treated (2 ng/ml) overnight. Cells were then incubated with 10
191 mg/ml cyclohexamide for 30 minutes prior to addition of 100 ng of EGF and incubated for the indicated
192 times. Cells were lysed directly in SDS-PAGE sample buffer (500 μl) and boiled, 35 μl was loaded on a 4-
193 12% NuPage gel for Western blot analysis.

194 **Cell activation.** The ability of IFN- γ to activate the phosphorylation of STAT1 was determined by
195 Western blot analysis. 4×10^5 cells/well were plated in a six well plate and cultured overnight. The cells
196 were either left untreated or treated with 100 ng/ml of the indicated IFN for 60 minutes. Cells were
197 lysed directly in SDS-PAGE sample buffer (500 μl) and boiled, 35 μl was loaded on a 4-12% NuPage gel
198 for Western blot analysis. All inhibitors were confirmed to be efficacious in HaCaT cells by evaluation of
199 the phosphorylation status of an appropriate protein as detailed in the figure legends. For evaluating
200 the activity of Stattic, IL6 (20 ng/ml) was added to the cells 15 minutes following the addition of Stattic.

201

202

203 **RESULTS**

204 **IFN- γ efficiently prevents HPV16 PsV infection**

205 We utilized HPV16 pseudovirus (PsV) infection to assess possible anti-viral effects of various
206 exogenous IFNs on the early stages of HPV infection. These experiments were performed in HaCaT cells,
207 a spontaneously transformed human keratinocyte cell line that is often utilized for PV entry analyses.
208 Treatment of cells with 10 ng/ml IFN- γ resulted in a dramatic decrease in HPV16 PsV infection, as
209 measured by expression of the GFP-encoding expression plasmid packaged by the PsV (Figure 1A).
210 Unexpectedly, treatment with 5 other IFN types, at the same concentration, did not affect PsV infection.
211 These negative results included several repeat experiments in which treatment with IFN- α and IFN- β ,
212 the IFN types reported previously to inhibit HPV16 PsV infection (6) were tested. For these experiments,
213 we used the same IFN source, cell line, and treatment time as in the earlier publication.

214 We next evaluated the dose dependence of IFN- γ on the inhibition of HPV16 PsV infection, by
215 performing a titration of the concentration of IFN- γ from 10 ng/ml to 3.2 pg/ml (Figure 1B). Infection
216 was inhibited even at low levels of exogenous IFN- γ , with substantial effects evident with a dose as low
217 as 0.08 ng/ml. Comparable levels can be present in the local environment during the course of a
218 microbial infection as occurs following herpes simplex type 2 infection of the vaginal tract (36)(37)(38).

219 IFN- γ exerts its effect on cells by engagement of its receptor, IFNGR, which typically activates
220 the Janus kinase (JAK)-signal transducer and activator of transcription (STAT) intracellular signal
221 transduction pathway, resulting in the transcriptional activation of IFN- γ -inducible genes (reviewed in
222 (39)). Inhibitors of this canonical signaling pathway include a pan-JAK inhibitor, Ruxolitinib, and a JAK2-
223 specific inhibitor, CEP-33779. In addition, IFN- γ may activate JAK-independent pathways. For example,
224 in response to IFN- γ , there may be activation of the signal transduction cascade that includes the
225 Mitogen-activated protein kinase kinase 1 (MEKK1), the Mitogen-activated protein kinase kinase 1
226 (MEK1), and the extracellular signal-regulated kinases 1 and 2 (ERK1/2), which regulate the

227 CCAAT/enhancer binding protein beta (C/EBP-beta) and C/EBP-beta-driven expression (40, 41). It has
228 also been shown that IFN- γ can trigger the phosphorylation of MEKK4 through activation of Pyk2 (FAK2)
229 in HaCaT cells (42). To determine which IFN- γ -induced pathway was responsible for the observed
230 reduction of HPV16 PsV infection, we treated HaCaT cells with inhibitors of these pathways prior to IFN-
231 γ addition and evaluated the subsequent effect on HPV16 PsV infection (Figure 1C). For this experiment,
232 we used a lower concentration of IFN- γ (0.2 ng/ml), which, because it inhibited infection less completely
233 than the higher concentration, made it possible to identify either an increase in infection, indicating that
234 the inhibitor blocked the IFN- γ pathway of interest, or a further reduction of infection, indicating the
235 inhibitor cooperated with the effects IFN- γ . None of the inhibitors had a dramatic effect on HPV16 PsV
236 infection in the absence of IFN- γ treatment, implying that under our normal growth conditions, PsV
237 infection does not utilize the pathways affected by the inhibitors (solid bars). In the presence of IFN- γ
238 (lined bars), none of the inhibitors augmented the anti-PsV activity of IFN- γ . However, the two JAK
239 inhibitors (Ruxolitinib, two concentrations shown, and CEP-33779) largely reversed the negative effect
240 of IFN- γ on PsV infection. These results indicate that the ability of IFN- γ to inhibit PsV infection depends
241 on the canonical JAK2/STAT1 pathway. By contrast, there was no effect on the IFN- γ -induced phenotype
242 when MEK1/2 was inhibited with U1026, FAK was inhibited with PF-573228, or STAT3 was inhibited by
243 Stattic, indicating that these pathways are not critical mediators of the reduction in PsV infection
244 induced by IFN- γ . The efficacy of these inhibitors in HaCaT cells at the chosen concentrations was
245 confirmed (Figure 1, panel E). The phosphorylation of FAK was incompletely blocked by PF-573228,
246 however we expect that this level of reduction would have been sufficient to be reflected in a functional
247 decrease (Figure 1, panel C).

248 To determine the stage of PsV infection that was the target of the observed antiviral effect, we
249 added IFN- γ to the HaCaT cells at different time points prior to or after HPV16 PsV addition (Figure 1D).
250 We found that we could still prevent almost 80% of PsV infection when we delayed addition of IFN- γ

251 until 3 hours post-pseudovirus addition. HPV exhibits a slow asynchronous entry with a half time of 4-11
252 hours. Thus, the inhibition kinetics led us to examine whether IFN- γ treatment affected the endocytic
253 entry of the pseudovirus.

254 **IFN- γ affects endocytic trafficking of HPV16 PsV**

255 To evaluate the possibility that IFN- γ treatment affects HPV16 entry in HaCaT cells, we
256 compared the localization of internalized HPV16 PsV at 24 hours post-infection in untreated cells with
257 those that were treated with IFN- γ , starting 18 hours prior to infection. Consistent with previous
258 studies, HPV16 L1 was localized in LE/lysosomes in the absence of IFN- γ (Figure 2A), and this pattern was
259 even more pronounced in the IFN- γ -treated cells (Figure 2B). IFN- γ treatment seemed to cause an
260 increase in the size of the LAMP-1-staining compartment in addition to the increased retention of PsV
261 capsids within this compartment. To examine this, we measured the diameter of 50 LE/lysosomes for
262 each condition. The range for untreated cells was 0.712 μm to 1.34 μm , with an average of 1.012 +/-
263 0.0201 μm . For IFN- γ treated cells the diameter range was 0.933 μm to 3.22 μm , with an average of
264 1.366 μm +/- 0.0579 (p value <0.0001). This increased size can also be appreciated in the inserted
265 panels shown in Figure 2A and 2B which shows the localization of HPV16 within the LAMP-1
266 compartment in both instances. We also examined the trafficking of the encapsidated pseudogenome,
267 using HPV16 PsV particles that had packaged an EdU-containing plasmid, which can localize the PV
268 pseudogenome during entry. At the 24 hour post-infection time point in untreated cells, most of the
269 genome had typically left the endosomal system. The residual vesicular genome colocalizes with L1
270 (Figure 2C). In contrast, the IFN- γ -treated cells demonstrated both increased retention of the genome
271 with L1, as well as stronger staining overall, probably indicating a decreased loss of genome during
272 capsid processing (Figure 2D). The inset panels in Figure 2C and 2D show a region shown at higher
273 magnification and the corresponding line profile at the bottom of the two panels verifies the

274 colocalization of the vesicular genome with L1 in both instances and the increased signal intensity in the
275 IFN- γ -treated condition.

276 The subcellular distribution of L2 ordinarily mirrors that of the pseudoviral DNA, as both of these
277 PsV components traffic together through the endosomes and TGN en route to ND10 (25). In untreated
278 cells, these components were colocalized and distributed among the endosomes, the TGN and ND10 at
279 the 24 hour time point, as previously described (Figure 2E) (22). By contrast, although L2 and the
280 pseudogenome were also colocalized in the IFN- γ -treated cells, there was no nuclear staining or Golgi-
281 like pattern (Figure 2F), all of the signal was apparently vesicular as also demonstrated by the staining
282 shown in panels 2B and 2D. The inserts in 2E and 2F contain a magnified region and the corresponding
283 line profile confirms an increased signal intensity following IFN- γ treatment. We also examined the
284 delivery of L2 to the Golgi complex. We have previously shown that L2 localizes to the TGN, adjacent to
285 the medial Golgi marker protein giantin, during infectious entry (22). This localization was readily seen
286 in the untreated cells (Figure 2G). In contrast, in the IFN- γ -treated cells, the distribution of L2 was
287 clearly distinct from the Golgi complex (Figure 2H). The inserted boxes show the single channel signals
288 for the indicated region. To further demonstrate the deficiency in L2 delivery to the Golgi, we quantified
289 the percentage of L2-positive cells that showed Golgi localization (100 L2+ cells were examined for each
290 condition). We found that only 13% of the IFN- γ treated cells, compared to 64% of the control cells, had
291 Golgi-localized L2. In sum, the microscopic analysis indicated that IFN- γ treatment caused the retention
292 of L2 and packaged DNA in the LE/lysosomal compartment, where they continued to be colocalized with
293 L1.

294 **IFN- γ treatment affects vesicular processing of HPV16 capsids but does not globally affect endocytic**
295 **trafficking**

296 The proteolytic processing of HPV16 capsids during cell entry, as recently analyzed in detail by
297 Cerqueira et al., results in distinct L1 cleavage products that are generated through protease cleavage
298 during endosomal trafficking (43). To determine if IFN- γ activation altered this process, we added
299 HPV16 PsV to untreated or IFN- γ -treated cells and examined L1 degradation during the initial 48 hours
300 of infection. We obtained similar results whether the L1 cleavage products were analyzed directly by
301 Western blot or immunoprecipitated with an anti-L1 polyclonal antiserum and then detected by
302 Western blotting with an anti-L1 monoclonal antibody. We focused on the
303 immunoprecipitation/Western procedure (Figure 3A), as this technique eliminates detection of the
304 multiple reactive cellular proteins in HaCaT cells that, as described by Cerqueira et al., can interfere with
305 analysis of the processed capsids by direct Western blotting (43). However, the heavy and light antibody
306 chains (labeled H and L, respectively) from the immunoprecipitation step are visible in all samples,
307 including the cell-only control. In untreated cells, as previously reported, a ladder of lower than full-
308 length L1-derived products, migrating between approximately 23 kDa and 45 kDa, was seen at the 6
309 hour time point, and these products were resolved at the 24 and 48 hour time points with the
310 coincident appearance of a lower product of approximately 15 kDa. In the IFN- γ -treated cells, however,
311 the processing was less extensive. The \sim 23 kDa doublet in the IFN- γ -treated cells was less prominent at
312 6 hours than in the untreated control at this time point, but the intensity of the doublet was increased
313 at 24 and 48 hours, making it similar to that of the untreated control at 6 hours and more intense than
314 the untreated control at the later time points. Furthermore, there was no decrease over time in the
315 slower migrating degradation products, and only a trace of the \sim 15 kDa product was seen. These results
316 indicate that the endocytic processing of HPV16 pseudovirions is impaired following IFN- γ treatment. It
317 should also be noted that this pattern does not resemble those observed previously with a panel of
318 protease inhibitors, nor does it resemble the pattern obtained following endosomal acidification

319 inhibition, in which generation of most of the L1 cleavage products required acidification, as the
320 appearance of the lower bands was prevented by either NH_4Cl or bafilomycin A treatment (43).

321 Given this L1 processing defect, we evaluated whether it might indicate a reduction in the
322 efficiency of the separation of L2 from the capsid which occurs prior to L2's egress from the LE/lysosome
323 (22, 44). Therefore, we determined the amount of L1-associated L2 at 24 hours post-infection in cells
324 that were untreated or $\text{IFN-}\gamma$ -treated, using immunoprecipitation of samples with an anti-L1 polyclonal
325 antiserum, followed by Western blotting for the detection of L1 and L2 proteins (Figure 3B). As
326 expected, HPV16 infection of untreated cells (lane 4), resulted in some full length L1 (upper panel) with
327 little associated L2 (lower panel), although there was ample capsid-associated L2 in the input capsids
328 (lane 2). As the L1-L2 dissociation occurs in a pH-dependent manner, the acidification inhibitor NH_4Cl
329 was included as a positive control for L2 retention (lane 5). When the cells were treated with $\text{IFN-}\gamma$ (lane
330 6), there was an increase in the amount of L2 that remained associated with L1 (compare with lane 4),
331 although it was less than seen with NH_4Cl treatment (compare with lane 5). Collectively, the data
332 indicate that HPV16 PsV processing/uncoating is incomplete in $\text{IFN-}\gamma$ -treated HaCaT cells. The result
333 does not phenotypically resemble that described for either protease inhibition or acidification inhibition.

334 There is substantial evidence that $\text{IFN-}\gamma$ plays diverse roles during modulation of endocytic
335 pathways (45) and results in the formation of enlarged endosomes in macrophages (46). Specific
336 endocytic-associated proteins induced by $\text{IFN-}\gamma$ that we deemed to be potential effectors included GILT
337 and Rab20. Rab20, functions in the maturation of phagocytic organelles, its expression was shown to be
338 induced by $\text{IFN-}\gamma$ in macrophages (47) and its overexpression induced the enlargement of the early
339 endosomal and LE compartments (48). However, in HaCaT cells, we did not observe an increase in
340 Rab20 expression following $\text{IFN-}\gamma$ treatment (data not shown). GILT was a second appealing effector
341 candidate; it is a $\text{IFN-}\gamma$ -inducible thiol reductase that catalyzes the disulfide bond reduction of proteins,
342 facilitating their further processing through cellular proteases (49, 50). As PV capsids are heavily

343 disulfide bonded, reductive processes could be involved in intracellular uncoating. GILT is present in
344 primary keratinocytes (51), but we found only low levels in HaCaT cells and no induction with IFN- γ (data
345 not shown), although control cells, melanoma cell lines SK-MEL-2 and SK-MEL-28, showed strong
346 induction, as expected (52). The increased expression of GILT in the melanoma cells did not correlate
347 with a decrease in HPV16 PsV infection; infection of SK-MEL-28 was actually substantially increased
348 following IFN- γ -treatment, whereas infection of SK-MEL-2 was decreased (data not shown). We
349 conclude that neither Rab20 nor GILT are effectors of the IFN- γ -induced depression of HPV16 PsV
350 infection.

351 We also determined if the effects observed for HPV16 capsid trafficking reflected a global
352 cellular perturbation in endocytic trafficking induced by IFN- γ activation. To address this issue, we
353 evaluated the entry of a cellular protein, transferrin receptor (TFR) and exogenous cargos with defined
354 trafficking routes. TFR is internalized from the plasma membrane into the early endosome with the
355 majority recycling to the plasma membrane and a subset continuing into lysosomes, where it is
356 degraded (53, 54). We examined the TFR distribution following overnight treatment with IFN- γ and
357 compared the steady state receptor distribution with untreated cells (Figure 4, panels A and B). IFN- γ
358 treatment did not induce a distinctive difference in the distribution of TFR, although its staining intensity
359 was clearly increased, probably indicating a minor kinetic perturbation. We also tracked the
360 internalization of the cargo protein, epidermal growth factor (EGF), which in association with its
361 receptor (EGFR), traffics from the plasma membrane to the late endosomal compartment via early
362 endosomes. EGF is degraded following internalization, whereas EGFR can be either recycled back to the
363 cell surface or degraded in lysosomes (55-57). We first examined the colocalization of EGF with the
364 early endosomal marker, EEA1, at both 30 minutes and 120 minutes following the addition of Alexa 488
365 coupled-EGF in the presence or absence of overnight treatment with IFN- γ prior to cargo addition
366 (Figure 4C-F). Unsurprisingly, partial colocalization of EGF with EEA1 was evident in the untreated cells

367 at 30 minutes (Figure 4C). At this early time point in the IFN- γ -treated cells, this colocalization was not
368 prevented, and was possibly slightly enhanced (Figure 4D). A more distinct difference was observed at
369 the later time point. In the untreated cells (Figure 4E), EGF was no longer localized to early endosomes,
370 and the fluorescent signal was reduced, presumably due to degradation. The IFN- γ -treated cells also
371 demonstrated a passage of EGF out of the early endosomes (Figure 4F), however, the intensity of the
372 EGF staining was not greatly reduced compared to the earlier time point. These results indicate that
373 EGF trafficking through the late endosomal compartment or lysosomal degradation may be affected by
374 IFN- γ treatment of HaCaT cells. We also evaluated the impact of IFN- γ treatment on the degradation of
375 EGFR following addition of EGF (Figure 3C). However, the appearance of lower molecular weight forms
376 of EGFR, indicating receptor processing, was similar in the presence or absence of IFN- γ , although a
377 possible slight delay in degradation following IFN- γ treatment may be seen in the 2 hour time point, as
378 indicated by the less intense lower band (Figure 3C, arrow). Thus, IFN- γ does not cause a dramatic
379 change in EGFR processing in HaCaT cells.

380 We examined two cargo proteins, cholera toxin B (CTXB) and ricin, that have been reported to
381 utilize the retromer complex to access to the trans Golgi network (TGN) from early endosomes (58-60).
382 The localization of Alexa 488 coupled-cholera toxin B (CTXB-488) was evaluated in cells that were
383 treated overnight with IFN- γ or untreated. CTXB-488 was allowed to internalize for 30 minutes to allow
384 substantial time to traffic into the TGN. It was clear that the IFN- γ treatment had no effect on the ability
385 of CTXB to enter the Golgi, as indicated by colocalization with giantin (compare Figure 4G [untreated]
386 and 4H [IFN- γ -treated]). Likewise, we evaluated the trafficking of Alexa 488-coupled ricin under these
387 conditions. There was also no effect on Golgi localization of ricin following a 30 minute incubation
388 (compare Figure 4I [untreated] and Figure 4J [IFN- γ -treated]). Thus, in HaCaT cells, retromer-dependent
389 trafficking from the early endosome to the Golgi is not disrupted by IFN- γ treatment.

390

391 **Sensitivity of other cell lines.**

392 All of the above analyses, except for the GILT control experiments with the melanoma cell lines,
393 were performed in HaCaT cells, a normal human skin-derived keratinocyte cell line. Therefore, we
394 determined if the observed effect could be observed in additional cell lines relevant for HPV studies
395 (Figure 5, panel A). HPV16 PsV infection of the 293TT cell line, which is an adenovirus transformed
396 human cell line used for HPV PsV propagation but is not considered a good system in which to study HPV
397 entry, was completely insensitive to IFN- γ treatment. HPV16 PsV infection of HeLa cells, which are
398 derived from an HPV18-positive cervical adenocarcinoma, showed an intermediate sensitivity to IFN- γ
399 treatment, with a maximum inhibition of less than 70%. Ect1 E6/E7, a cell line derived from normal
400 human ectocervical epithelium that had been immortalized by expression of HPV16 E6/E7, showed
401 complete inhibition of HPV16 PsV infection following IFN- γ treatment. However, this line was less
402 sensitive than HaCaT cells, with the inhibition dropping off sharply in Ect1 E6/E7 at progressively lower
403 concentrations than 2 ng/ml, in contrast to HaCaT. We also examined the sensitivity of HPV16 PsV
404 infection of a murine keratinocyte cell line, S1, to murine IFN- γ treatment. This cell line demonstrated
405 low sensitivity to the treatment, with a maximum inhibition of 40%. We verified that all of these cell
406 lines could respond to IFN- γ by confirming the appearance of the phosphorylated form of STAT1 in
407 response to IFN- γ treatment (Figure 5, panel B, lower part). The upper portion of this panel shows the
408 detection of endogenous STAT1. Therefore, all cell lines were clearly responsive to IFN- γ , despite the
409 observed differences of this treatment on HPV16 PsV infection. Importantly, it is clear that the IFN-
410 γ phenotype is not confined to the HaCaT cell line.

411

412 **HPV genera are differentially affected by IFN- γ treatment.**

413 To see if the IFN- γ sensitivity of HPV16 PsV extended to other HPV types, we compared the
414 infection of HaCaT cells, either untreated or treated overnight with IFN- γ , by seventeen additional HPV

415 PsV types, including alpha and beta genera members. HPV16 is a genus alpha, species 9 member, and
416 we analyzed four additional species alpha-9 members; HPV31, HPV33, HPV52 and HPV58 (Figure 6,
417 panel A). Infection with three of the alpha-9 members was strongly inhibited by IFN- γ treatment
418 (HPV31, HPV52, and HPV58), but HPV33 showed only an intermediate sensitivity, with approximately
419 50% maximum inhibition. The alpha-8, HPV40, and alpha-11, HPV73, representatives also showed
420 strong inhibition of infection (Figure 6, panel B), whereas two alpha-10 members, HPV6 and HPV11,
421 were only weakly inhibited. We examined five members of the alpha-7 species; HPV18, HPV39, HPV59,
422 HPV45 and HPV68 (Figure 6, panel C), and observed approximately 80% inhibition of HPV18 infection,
423 but the other species members were not strongly affected by IFN- γ treatment. HPV39 and HPV45 were
424 particularly insensitive. Additionally, an alpha-5 representative, HPV26, was poorly inhibited. We also
425 determined the inhibition profile of three genus beta members: species beta-1 members HPV5 and
426 HPV8, and the beta-2 type HPV38. Infection of all three types was strongly inhibited by IFN- γ treatment
427 (Figure 6, panel D). We also examined the sensitivity of three animal PV types: BPV1, CRPV and MusPV1.
428 Infection of BPV1 and CRPV was strongly inhibited (more than 80% inhibition), whereas inhibition of
429 MusPV1 was intermediate (approximately 40% maximum inhibition) (data not shown). Thus, the
430 sensitivity to IFN- γ is not limited to HPV16, to alpha-9 species members, nor to human PV types.
431 However, the relative insensitivity of four of the five tested alpha-7 types is especially intriguing. This
432 data also reinforces the conclusion that IFN- γ treatment does not globally inhibit endosomal trafficking
433 in HaCaT cells, as such an effect would have been predicted to affect all PV types equally as no studies
434 have proven the utilization of distinct entry pathways for different HPV types (34, 61, 62).

435

436 **IFN- γ sensitivity correlates with L2 type.**

437 Given the heterogeneity of the various HPV types to inhibition by IFN- γ treatment, we reasoned
438 that it might be possible to determine whether the sensitivity of a given HPV type was attributable to its

439 L1 or L2 protein, through the analysis of hybrid L1/L2 infectious PsV whose capsid proteins were derived
440 from HPV types that differ in their sensitivity to IFN- γ . It is known that, for some PV types, it is possible
441 to exchange the two capsid proteins between two different types and obtain intact, assembled particles.
442 For instance, HPV11 L1 was found to form complexes with L2 proteins from a variety of other HPV types,
443 including non-alpha-10 types and even with the animal type, COPV1 (63). We found that infectious PsV
444 can be produced from some, but not all, capsid protein combinations (unpublished data and Figure 7A).
445 To determine if the disparate IFN- γ effects observed for the various HPV types could be attributed to
446 either of the individual capsid proteins, we produced infectious hybrid particles between HPV45 L1 as
447 the type insensitive to IFN- γ treatment, and HPV16 L2 as the sensitive type (termed HPV45/16). The
448 inverse combination (HPV16/45) did not produce infectious particles, although co-assembly was robust
449 (data not shown). HPV 45/16 PsV infection was inhibited by IFN- γ treatment whereas the IFN- γ
450 responses of HPV16 L1/L2 and HPV45 L1/L2 were, respectively, sensitive and insensitive, as expected
451 (Figure 7A). As the IFN- γ -sensitive capsid protein in the hybrid PsV was derived from HPV16 L2, this
452 result suggests that the L2 protein determines the IFN- γ sensitivity phenotype of the HPV. Given that
453 HPV 16/45 PsV did not result in infectious particles, we produced hybrid PsV from a different
454 combination of PV capsid proteins to test the hypothesis that IFN- γ sensitivity maps to the L2 protein.
455 Hybrid particles from HPV45 and HPV18, two alpha-7 types that displayed opposite phenotypes in
456 response to treatment, were assembled. Fortuitously, in this instance both hybrid combinations
457 resulted in infectious PsV. The results with these hybrids confirmed that L2 mediates the sensitivity to
458 IFN- γ , as the HPV 45/18 hybrid, whose L2 is from the IFN- γ -sensitive HPV18, was inhibited by IFN- γ , while
459 the HPV 18/45 hybrid, whose L2 is from the IFN- γ -insensitive HPV45, was resistant to IFN- γ (Figure 7B).
460 Different HPV PsV types can have different L1/L2 ratios and also exhibit various particle to
461 infectivity ratios, and the two can only be partially correlated (34). To confirm that the differential
462 effects of IFN- γ that we observed were not attributable to a trivial explanation, such as the level of L2

463 incorporation or purity of particle preparation, all PsV were analyzed by SDS-PAGE electrophoresis and
464 Coomassie G-250 staining (Figure 7C). Although there was a range of incorporated L2 levels among
465 these preparations, with L2 being undetectable in some instances, there was no obvious correlation
466 with either L2 incorporation or PsV purity and IFN- γ sensitivity. As an example, an L2 band is clearly
467 evident for HPV26, HPV39, HPV59 and HPV68, all IFN- γ insensitive types. L2 is equally obvious for HPV5,
468 HPV8, HPV38, HPV40, HPV52 and HPV73, IFN- γ sensitive types.

469

470 **DISCUSSION**

471 The IFN family plays a pivotal role in the control of many viral infections and in shaping the
472 subsequent adaptive immune response. Their actions are mediated through signaling pathways
473 triggered by the engagement of receptors that activate the expression of IFN-stimulated genes (ISGs).
474 Each IFN induces a distinct ISG profile that includes both shared and unique members (64, 65). These
475 ISG proteins can exert, among numerous other activities, antiviral actions that can target vulnerabilities
476 at all the stages of the viral life cycle, including entry, transcription, translation, genome replication,
477 assembly, and egress (reviewed in (66)), although the described effects of most reports have concluded
478 that the inhibition is largely at the level of viral transcription and translation, including studies on the
479 structurally-related polyomaviruses (67, 68). The identified effector molecules in these studies include
480 RNA-dependent protein kinase (PKR), adenosine deaminase (ADAR), guanylate-binding proteins (GBP1
481 and GBP2), and nitric oxide synthetase (NOS), although in other instances the observed effects are
482 unascrbed (69-75).

483 We initiated this study to evaluate the entry step at which type I IFNs, both IFN- α and IFN- β ,
484 inhibited HPV16 PsV infection of HaCaT cells, which had been described by Warren et al (6). However,
485 we were unable to observe an effect of type I IFN on HPV16 PsV infection, despite repeated attempts
486 with reagents from various sources, including the same source, treatment time, and concentration

487 utilized in the previous study. The only clear distinction between the protocols is that we utilized a GFP
488 reporter system which allows determination of the number of infected cells, after gating on only living
489 cells, whereas the previous study used a luciferase reporter. In that assay system, the luciferase signal is
490 obtained from the lysate of the entire cell population which would include cells adversely affected by
491 the treatment. This difference could explain the disparate results. Indeed, when we performed an
492 inhibition assay using HPV16 PsV containing a dual luciferase/GFP reporter plasmid, we observed
493 inhibition in the luciferase assay, comparable to that previously reported, but not in the GFP flow
494 cytometric assay (unpublished data).

495 Given that we have evaluated PsV, our results do not address the possibility that type I IFNs
496 might influence later aspects of the viral life cycle, as would be predicted from the observation that the
497 viral oncoproteins actively inhibit IFN-mediated cellular responses (76-79) and numerous studies have
498 demonstrated the efficacy of type I interferon in the clearance of episomal HPV genomes (80, 81).

499 In contrast to type I IFNs, we observed a dramatic abrogation of HPV16 PsV infection following
500 IFN- γ treatment, which had not been examined previously. This inhibition was mediated through the
501 canonical JAK/STAT pathway although type I IFN treatment can also induce this pathway in HaCaT cells
502 ((82) and data not shown) therefore, the critical induction downstream of this activation is not shared
503 between these treatments. Interestingly, the inhibition of infection occurred at the level of virus entry
504 and trafficking, prior to nuclear delivery of the viral genome. Based on our microscopic and biochemical
505 analysis, endosomal capsid processing was affected, proteolytic digestion of L1 was incomplete and L2
506 was not resolved from the capsid complex as typically occurs during PV uncoating. This processing block
507 did not mimic that observed following neutralization of the endosomes or inhibition of essential
508 proteases as previously reported (43).

509 A parallel IFN- γ effect was reported for influenza A, where it was found that the incoming viral
510 particles were sequestered in an expanded LE compartment and viral fusion was prevented. However,

511 this effect was attributable to induction of IFITM3 (83), which has been convincingly demonstrated to
512 have no effect on HPV16 PsV infection (6), therefore this mechanism is unlikely to be mediating the
513 effects described here. Other IFN- γ -induced effector molecules that are known to affect the endosomal
514 compartment include Rab20 and GILT (47-50) but our analyses lead us to conclude that neither protein
515 makes a major contribution to the inhibition of HPV16 PsV infection.

516 Although the normal endosomal processing of HPV16 capsids was prevented in the IFN- γ treated
517 cells, we demonstrated by both biochemical and microscopic methods that vesicular processing was not
518 globally affected. Therefore, it is unlikely that our observations reflect a general inhibition of endosomal
519 degradation or severe cellular perturbation. Further supporting this conclusion are the data that some
520 HPV types were impervious to IFN- γ activation and distinct entry pathway usage for various PVs has not
521 been demonstrated (61, 62). No HPV PsV types have been described to be resistant to either furin
522 inhibition or gamma secretase inhibition, which reflect both extracellular and intracellular processing
523 requirements, although differences in cell surface interactions have been described (13, 16, 34). The
524 effect of IFN- γ treatment on the endosomal pH and protein processing has been well documented in
525 macrophages. These studies have concluded that IFN- γ treatment does not result in less efficient
526 acidification or change the proteolytic activity of the lysosomal/phagosomal compartments (84-86).
527 However, as these studies were all performed in macrophages, we could not assume that IFN- γ
528 activation of HaCaT cells did not affect endosomal pH. It has been well established that PVs require
529 passage through the low pH environment of the LE for infection (13). However, as we observed
530 differences among HPV types in their sensitivity to IFN- γ , we wanted to ensure that this heterogeneity
531 was not associated with subtle differences in pH dependence. We performed a titration of both
532 bafilomycin A and NH₄Cl, which indicated that all members of a panel of sensitive and resistant types
533 were equally sensitive to the pharmacologically-induced higher pH (data not shown).

534 One of the interesting facets of our study is the observation that PsV inhibition is mediated
535 through the L2 protein. As previously mentioned, L2 segregates with the viral DNA from L1 during
536 endocytosis. This segregation is pH dependent and is mediated, at least in part, by the action of
537 cyclophilins (44). Our biochemical and fluorescent analyses indicate that IFN- γ treatment prevents this
538 dissociation event. To evaluate if IFN- γ interferes with the action of cyclophilins, we assessed the
539 susceptibility of a panel of PsV, including those most sensitive and most insensitive to IFN- γ , to
540 cyclosporine A (CSA), a cyclophilin inhibitor. We found no correlation between these profiles, as a
541 specific example, HPV45, a type relatively impervious to IFN- γ , was inhibited with CSA to the same
542 extent as HPV16 (data not shown).

543 As shown, some genera seem to be resistant to treatment. The sensitivity phenotype is roughly
544 correlative with genotype but there are notable exceptions, e.g. HPV18 is the sole sensitive alpha 7
545 member. This observation indicates that aspects of the uncoating process, at the level of L2/genome
546 dissociation from L1, must differ across the HPV lineage or at least among HPV types. Type-specific
547 differences in uncoating have not been previously described. Identification of the critical ISG or
548 interferon regulated gene (IRG), as the observed effect could also be due to downregulation of an
549 essential protein, will be instrumental in understanding this aspect of HPV intracellular trafficking. This
550 information could explain why some HPV types are resistant and possibly indicate how the various types
551 differ in the critical step of L2/DNA segregation from the endocytosed capsid.

552

553 **Acknowledgements:** We thank Richard Roden and Joshua Wang from Johns Hopkins University and
554 Martin Müller from DKFZ-Heidelberg for the generous sharing of reagents. We also thank the CCR-NCI-
555 NIH confocal core facility for access to their facilities. Research was supported by the Intramural
556 Research Program of the National Institutes of Health, National Cancer Institute, Center for Cancer
557 Research.

558 **FIGURE LEGENDS**

559 **Figure 1. HPV16 PsV infection of HaCaT cells is sensitive to type II IFN treatment. (A)** HaCaT cells were

560 treated with 10 ng/ml of various types of IFN for 18 hours prior to infection with an HPV16 PsV that

561 contained a packaged GFP expression plasmid. GFP expression was determined by flow cytometric

562 analysis at 72 hours post-infection. The percent of infection in untreated cells was set to 100%. The

563 percent of infection in the treated samples was normalized to that value. Triplicate infections were

564 analyzed for all experiments. **(B)** The amount of IFN- γ necessary to decrease HPV16 PsV infection was

565 determined by titration. The noted amount of IFN- γ was added to cells 18 hours prior to

566 commencement of infection. Inhibition data was normalized to untreated, infected cells. **(C)** Inhibitors

567 were added immediately prior to IFN- γ addition (0.2 ng/ml) or analyzed in the absence of activation.

568 The unlined bars indicate the infection with the inhibitor only and the lined bars in the same color shade

569 indicate the data with IFN- γ activation. The data are normalized to the infection levels in HPV16 PsV

570 untreated, infected cells. The inhibitors were used at the following concentrations: PF-573228, 100 nM;

571 Ruxolitinib 1, 1 μ M and 100 nM, Ruxolitinib 2; U1026, 100 nM; CEP-33779, 20 nM; C16, 1 μ M, Stattic 1

572 μ M. As noted in the text, only treatment with Ruxolitinib and CEP-33779 repressed the IFN- γ effect on

573 HPV16 PsV infection. **(D)** 5 ng/ml of IFN- γ was added at different times pre- or post-infection with

574 HPV16 PsV, as indicated and infection data normalized to untreated, infected cells. **(E)** The efficacy of

575 the inhibitors at the concentrations utilized for panel C were evaluated by examination of the

576 phosphorylation status of the target protein as indicated. To induce STAT3 phosphorylation cells were

577 treated with 20 ng of IL6 for 15 minutes following addition of Stattic. Both concentrations of Ruxolitinib

578 shown in panel C and were evaluated for their ability to block STAT1 phosphorylation. A lower

579 concentration (10 nM) was found to be inefficient.

580

581 **Figure 2. Viral components do not exit the LE in IFN- γ -treated cells.** The localization of HPV16 PsV
582 components were compared in untreated HaCaT cells and IFN- γ -treated cells at 24 hours post-infection.
583 IFN- γ -treated cells were treated for 18 hours prior to virus addition. In all instances, the IFN- γ -treated
584 condition is shown in the second panel of the pair. Panels A and B show the staining of HPV16 L1 in the
585 green channel and the lysosomal protein LAMP-1 in the red channel. Note the increased staining
586 intensity and colocalization in the IFN- γ -treated cells (panel B). The inset in each of these panels shows a
587 surface rendered image of a Z-stack series of each condition. Panels C and D show the localization of the
588 delivered PsV genome in the green channel and L1 protein in the red channel. In order to appreciate the
589 intensity of the vesicular staining in each condition, we have examined a line profile across a 7 μ M
590 region and inserted this within the panel along with a magnification of this region. The y-axis reflects
591 the pixel intensity across the distance (x-axis). The third group, shown in panels E and F, show the
592 colocalization of the PsV genome (green) and L2 protein (red). The line profiles for a chosen region have
593 been inserted. In the final group (panels G and H), the Golgi localization of L2 was evaluated by co-
594 staining of L2 (green) with giantin (red). A split image of a chosen region is shown to allow better
595 appreciation of the localization of L2 staining relative to the medial Golgi marker.

596

597 **Figure 3. Intracellular processing in the presence of IFN- γ .** (A) The intracellular processing of HPV16
598 L1 was examined by anti-L1 VLP immunoprecipitation using a rabbit polyclonal antiserum followed by
599 Western blotting using a monoclonal antibody in both untreated and IFN- γ -treated HaCaT cells. In the
600 uninfected, cells only conditions, indicated by "co", only the heavy and light chain antibody bands were
601 evident (indicated H and L). In the HPV16 PsV infected cells the full length, unprocessed L1 band (FL)
602 was evident throughout the time course. Lower molecular weight products, migrating between 23 kDa
603 and 45 kDa, were evident by 6 hours in the untreated cell conditions. The 23 kDa band and an
604 additional 15 kDa band were evident at the 24 hour and 48 hour time points. In the IFN- γ -treated

605 conditions, the intermediate sized products did not resolve throughout the time course and little
606 accumulation of the 15 kDa band occurred. **(B)** The separation of the minor capsid protein, L2 from the
607 major capsid protein, L1 was evaluated in untreated and IFN- γ -treated cells at 24 hours post-infection.
608 Uninfected cells (lane 3) or HPV16 PsV infected cells (lanes 4 untreated, lane 5 NH₄Cl-treated, lane 6 IFN-
609 γ -treated) were immunoprecipitated with rabbit anti-L1 VLP antiserum and the presence of the two
610 capsid proteins were evaluated by Western blotting with mouse monoclonal antibodies (L1 in top panel,
611 L2 in bottom panel). Lane 2 shows the migration of the input virion proteins. The lower band in lane 2
612 in the anti-L1 blot is the full length L1 protein, the upper band indicates cross reaction of this antibody
613 with the L2 protein. Most of the lower molecular weight L1 products shown in panel B were cropped
614 out of this figure, but some of the weak, upper bands are evident in lanes 5 and 6. Following NH₄Cl
615 treatment (lane 5), there was an increase in L1 and L1-associated L2. This was also evident, to a lesser
616 degree, in the IFN- γ -treated condition (lane 6). **(C)** The intracellular processing of EGFR following EGF
617 addition was examined in either untreated HaCaT cells or in IFN- γ -treated cells (18 hours pretreatment)
618 by Western blot analysis. The appearance of lower molecular weight forms of EGFR was similar in both
619 conditions (arrow). The lower panel demonstrates equivalent protein concentrations by the comparison
620 of GAPDH levels.

621

622 **Figure 4. Effect of IFN- γ -treatment on protein trafficking.** HaCaT cells were untreated or treated with
623 IFN- γ for 18 hours. The untreated conditions are shown in the left column and the IFN- γ -treated
624 conditions are in the right column. The steady state distribution of the transferrin receptor (TFR) was
625 examined and is shown in panel A (untreated) and panel B (treated). The delivery of Alexa 488-coupled
626 epidermal growth factor (EGF, green channel) to early endosomes, as indicated by anti-EEA1 staining
627 (red channel) was examined at two time points following EGF addition; 30 minutes shown in panels C
628 (untreated) and panel D (treated), and 2 hours shown in E (untreated) and panel F (treated). Please

629 note that the slightly increased EGF signal at the 2 hour time point does not colocalize with EEA1. For
630 each panel a selected region is shown as a split image within each panel. The Golgi delivery of the
631 retromer-dependent cargoes; Alexa 488-coupled Cholera Toxin B (CTXB-488) and FITC-coupled ricin
632 (green channel) was determined by colocalization with giantin (red channel) is shown in panels G-J.
633 Delivery of both reagents was examined at 30 minutes post-addition. For each panel a selected region is
634 shown as a split image within the panels; untreated cells are shown in panel G (CTXB) and panel I (ricin)
635 and IFN- γ -treated cells are shown in panel H (CTXB) and panel J (ricin).

636

637 **Figure 5. Evaluation of IFN- γ -treatment of other cell lines.** (A) To determine the IFN- γ sensitivity of
638 HPV16 PsV infection in additional cell lines, we pretreated a panel of cell lines with the indicated
639 concentration for 18 hours prior to HPV16 PsV addition. GFP-positive cells were determined at 72 hours
640 post-infection and normalized to the untreated, infected population. The S1 cell line was treated with
641 murine IFN- γ . Triplicate infections were analyzed for all experiments. (B) The ability of these cells lines
642 to respond to IFN- γ treatment was determined by Western blot analysis of endogenous form of STAT1
643 (upper panel) and the appearance of the tyrosine 701 phosphorylated form of STAT1 (lower panel). The
644 inclusion of IFN- γ is indicated by the + above the appropriate lane. Note that all cell lines have an intact
645 IFN- γ activation capacity.

646

647 **Figure 6. Susceptibility of other HPV types to IFN- γ treatment.** To determine if other HPV types also
648 showed a sensitivity to IFN- γ treatment, we examined the infection of a panel of HPV PsV types on
649 HaCaT cells. All PsV types were initially titrated to determine the PsV amount to generate 15-30%
650 infected cells. This amount was then used to infect untreated cells and cells that had been treated with
651 a titration series of IFN- γ . The percentage of inhibition was determined by normalizing to the untreated
652 control infection. The species groupings are indicated above each panel and next to the HPV type

653 indicated in the panel legend. Alpha 9 species members are shown in panel A; alpha 8, 10 and 11 in
654 panel B; alpha 5 and 7 in panel C; and beta 1 and 2 members are shown in panel D. Triplicate infections
655 were analyzed for all experiments.

656

657 **Figure 7. The HPV type of the L2 protein confers IFN- γ response phenotype.** Hybrid HPV PsVs were
658 assembled and infectivity was confirmed by titration on HaCaT cells. The PsV amount to confer 15-35%
659 infection was then used to evaluate the sensitivity to IFN- γ . **(A)** Both HPV16 and HPV45 displayed their
660 previously demonstrated infection phenotype following IFN- γ treatment. The hybrid PsV that contained
661 the HPV45 L1 protein and the HPV16 L2 protein shared the sensitivity of the HPV16 PsV to IFN-
662 γ treatment. **(B)** Hybrid PsV were assembled to contain HPV45 L1 and HPV18 L2 and the inverse shuffle,
663 HPV18 L1 and HPV45 L2. The former capsid combination was sensitive to IFN- γ treatment, like the
664 HPV18/18 PsV. The latter PsV, with HPV45 L2, was not sensitive to IFN- γ treatment, resembling the
665 HPV45/45 PsV. **(C)** The capsid composition and purity was determined for each PsV type. Purified
666 particles were examined by Coomassie G-250 staining. The dominant band in each type is the L1
667 protein, the more slowly migrated band evident in some types is the L2 protein. HPV18 and HPV45 PsV
668 preparations that were generated with the bicistronic expression plasmid and the two separate L1 and
669 L2 expression plasmids are both shown.

670

671

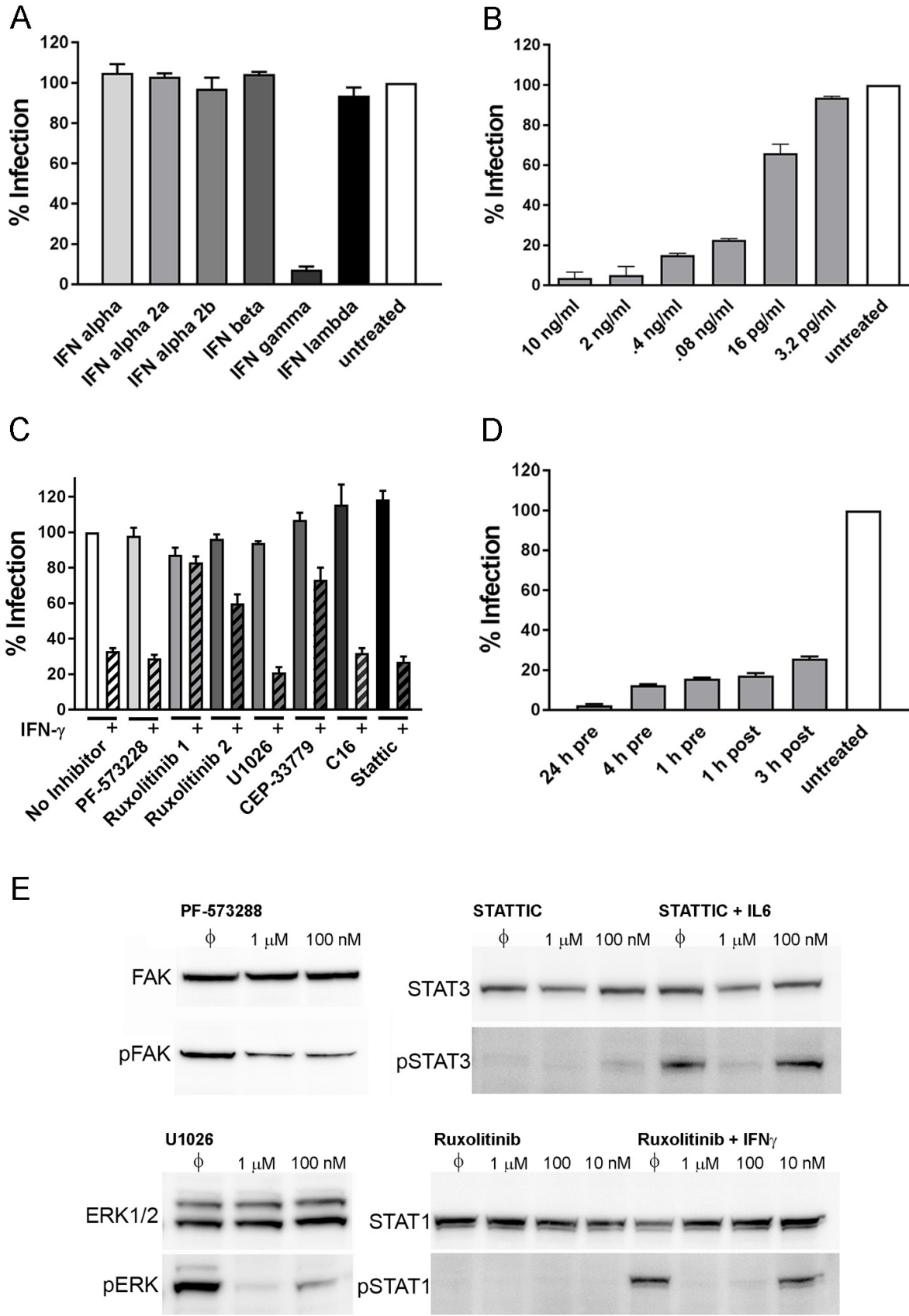
- 672 1. **Plummer M, de Martel C, Vignat J, Ferlay J, Bray F, Franceschi S.** 2016. Global burden of
673 cancers attributable to infections in 2012: a synthetic analysis. *Lancet Glob Health* **4**:e609-616.
- 674 2. **Howley PM SJ, Lowy DR** 2013. Papillomaviruses, p. 1662-1703, *Fields Virology*. Lippincott
675 Williams & Wilkins, Philadelphia.
- 676 3. **Stanley M.** 2010. HPV - immune response to infection and vaccination. *Infect Agent Cancer* **5**:19.
- 677 4. **Frazer IH.** 2009. Interaction of human papillomaviruses with the host immune system: a well
678 evolved relationship. *Virology* **384**:410-414.
- 679 5. **Vedham V, Divi RL, Starks VL, Verma M.** 2014. Multiple infections and cancer: implications in
680 epidemiology. *Technol Cancer Res Treat* **13**:177-194.
- 681 6. **Warren CJ, Griffin LM, Little AS, Huang IC, Farzan M, Pyeon D.** 2014. The antiviral restriction
682 factors IFITM1, 2 and 3 do not inhibit infection of human papillomavirus, cytomegalovirus and
683 adenovirus. *PLoS One* **9**:e96579.
- 684 7. **Isaacs A, Lindenmann J.** 1957. Virus interference. I. The interferon. *Proc R Soc Lond B Biol Sci*
685 **147**:258-267.
- 686 8. **Stark GR, Kerr IM, Williams BR, Silverman RH, Schreiber RD.** 1998. How cells respond to
687 interferons. Annual review of biochemistry **67**:227-264.
- 688 9. **de Weerd NA, Nguyen T.** 2012. The interferons and their receptors--distribution and regulation.
689 *Immunol Cell Biol* **90**:483-491.
- 690 10. **Kotenko SV, Gallagher G, Baurin VV, Lewis-Antes A, Shen M, Shah NK, Langer JA, Sheikh F,
691 Dickensheets H, Donnelly RP.** 2003. IFN-lambdas mediate antiviral protection through a distinct
692 class II cytokine receptor complex. *Nat Immunol* **4**:69-77.
- 693 11. **Buck CB, Pastrana DV, Lowy DR, Schiller JT.** 2004. Efficient intracellular assembly of
694 papillomaviral vectors. *J Virol* **78**:751-757.
- 695 12. **Sapp M, Day PM.** 2009. Structure, attachment and entry of polyoma- and papillomaviruses.
696 *Virology* **384**:400-409.
- 697 13. **Day PM, Schelhaas M.** 2014. Concepts of papillomavirus entry into host cells. *Current opinion in
698 virology* **4**:24-31.
- 699 14. **Joyce JG, Tung JS, Przysiecki CT, Cook JC, Lehman ED, Sands JA, Jansen KU, Keller PM.** 1999.
700 The L1 major capsid protein of human papillomavirus type 11 recombinant virus-like particles
701 interacts with heparin and cell-surface glycosaminoglycans on human keratinocytes. *J Biol Chem*
702 **274**:5810-5822.
- 703 15. **Giroglou T, Florin L, Schafer F, Streeck RE, Sapp M.** 2001. Human papillomavirus infection
704 requires cell surface heparan sulfate. *J Virol* **75**:1565-1570.
- 705 16. **Johnson KM, Kines RC, Roberts JN, Lowy DR, Schiller JT, Day PM.** 2009. Role of heparan sulfate
706 in attachment to and infection of the murine female genital tract by human papillomavirus. *J
707 Virol* **83**:2067-2074.
- 708 17. **Richards RM, Lowy DR, Schiller JT, Day PM.** 2006. Cleavage of the papillomavirus minor capsid
709 protein, L2, at a furin consensus site is necessary for infection. *Proc Natl Acad Sci U S A*
710 **103**:1522-1527.
- 711 18. **Kines RC, Thompson CD, Lowy DR, Schiller JT, Day PM.** 2009. The initial steps leading to
712 papillomavirus infection occur on the basement membrane prior to cell surface binding. *Proc
713 Natl Acad Sci U S A* **106**:20458-20463.
- 714 19. **Schelhaas M, Shah B, Holzer M, Blattmann P, Kuhling L, Day PM, Schiller JT, Helenius A.** 2012.
715 Entry of human papillomavirus type 16 by actin-dependent, clathrin- and lipid raft-independent
716 endocytosis. *PLoS Pathog* **8**:e1002657.
- 717 20. **Selinka HC, Giroglou T, Sapp M.** 2002. Analysis of the infectious entry pathway of human
718 papillomavirus type 33 pseudovirions. *Virology* **299**:279-287.

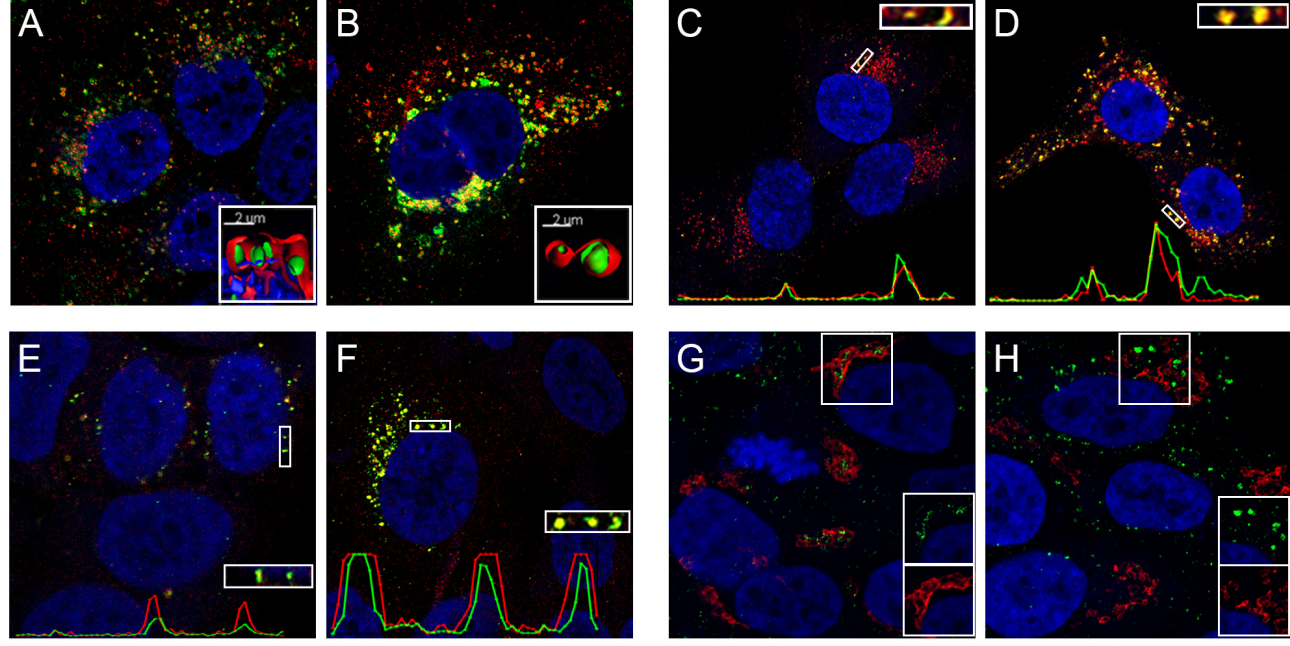
- 719 21. **Day PM, Lowy DR, Schiller JT.** 2003. Papillomaviruses infect cells via a clathrin-dependent
720 pathway. *Virology* **307**:1-11.
- 721 22. **Day PM, Thompson CD, Schowalter RM, Lowy DR, Schiller JT.** 2013. Identification of a role for
722 the trans-Golgi network in human papillomavirus 16 pseudovirus infection. *J Virol* **87**:3862-3870.
- 723 23. **Lipovsky A, Popa A, Pimienta G, Wyler M, Bhan A, Kuruvilla L, Guie MA, Poffenberger AC,**
724 **Nelson CD, Atwood WJ, DiMaio D.** 2013. Genome-wide siRNA screen identifies the retromer as
725 a cellular entry factor for human papillomavirus. *Proc Natl Acad Sci U S A* **110**:7452-7457.
- 726 24. **Popa A, Zhang W, Harrison MS, Goodner K, Kazakov T, Goodwin EC, Lipovsky A, Burd CG,**
727 **DiMaio D.** 2015. Direct binding of retromer to human papillomavirus type 16 minor capsid
728 protein L2 mediates endosome exit during viral infection. *PLoS Pathog* **11**:e1004699.
- 729 25. **Day PM, Baker CC, Lowy DR, Schiller JT.** 2004. Establishment of papillomavirus infection is
730 enhanced by promyelocytic leukemia protein (PML) expression. *Proc Natl Acad Sci U S A*
731 **101**:14252-14257.
- 732 26. **Pyeon D, Pearce SM, Lank SM, Ahlquist P, Lambert PF.** 2009. Establishment of human
733 papillomavirus infection requires cell cycle progression. *PLoS Pathog* **5**:e1000318.
- 734 27. **Boukamp P, Petrussevska RT, Breitkreutz D, Hornung J, Markham A, Fusenig NE.** 1988. Normal
735 keratinization in a spontaneously immortalized aneuploid human keratinocyte cell line. *The*
736 *Journal of cell biology* **106**:761-771.
- 737 28. **Suh KS, Mutoh M, Nagashima K, Fernandez-Salas E, Edwards LE, Hayes DD, Crutchley JM,**
738 **Marin KG, Dumont RA, Levy JM, Cheng C, Garfield S, Yuspa SH.** 2004. The organellular chloride
739 channel protein CLIC4/mtCLIC translocates to the nucleus in response to cellular stress and
740 accelerates apoptosis. *J Biol Chem* **279**:4632-4641.
- 741 29. **Roden RB, Greenstone HL, Kirnbauer R, Booy FP, Jessie J, Lowy DR, Schiller JT.** 1996. In vitro
742 generation and type-specific neutralization of a human papillomavirus type 16 virion
743 pseudotype. *J Virol* **70**:5875-5883.
- 744 30. **Day PM, Pang YY, Kines RC, Thompson CD, Lowy DR, Schiller JT.** 2012. A human papillomavirus
745 (HPV) in vitro neutralization assay that recapitulates the in vitro process of infection provides a
746 sensitive measure of HPV L2 infection-inhibiting antibodies. *Clinical and vaccine immunology :*
747 *CVI* **19**:1075-1082.
- 748 31. **Rubio I, Seitz H, Canali E, Sehr P, Bolchi A, Tommasino M, Ottonello S, Muller M.** 2011. The N-
749 terminal region of the human papillomavirus L2 protein contains overlapping binding sites for
750 neutralizing, cross-neutralizing and non-neutralizing antibodies. *Virology* **409**:348-359.
- 751 32. **Chen JW, Murphy TL, Willingham MC, Pastan I, August JT.** 1985. Identification of two lysosomal
752 membrane glycoproteins. *The Journal of cell biology* **101**:85-95.
- 753 33. **Cardone G, Moyer AL, Cheng N, Thompson CD, Dvoretzky I, Lowy DR, Schiller JT, Steven AC,**
754 **Buck CB, Trus BL.** 2014. Maturation of the human papillomavirus 16 capsid. *MBio* **5**:e01104-
755 01114.
- 756 34. **Kwak K, Jiang R, Wang JW, Jagu S, Kirnbauer R, Roden RB.** 2014. Impact of inhibitors and L2
757 antibodies upon the infectivity of diverse alpha and beta human papillomavirus types. *PLoS One*
758 **9**:e97232.
- 759 35. **Day PM, Thompson CD, Buck CB, Pang YY, Lowy DR, Schiller JT.** 2007. Neutralization of human
760 papillomavirus with monoclonal antibodies reveals different mechanisms of inhibition. *J Virol*
761 **81**:8784-8792.
- 762 36. **Milligan GN, Bernstein DI.** 1997. Interferon-gamma enhances resolution of herpes simplex virus
763 type 2 infection of the murine genital tract. *Virology* **229**:259-268.
- 764 37. **Parr MB, Parr EL.** 1999. The role of gamma interferon in immune resistance to vaginal infection
765 by herpes simplex virus type 2 in mice. *Virology* **258**:282-294.

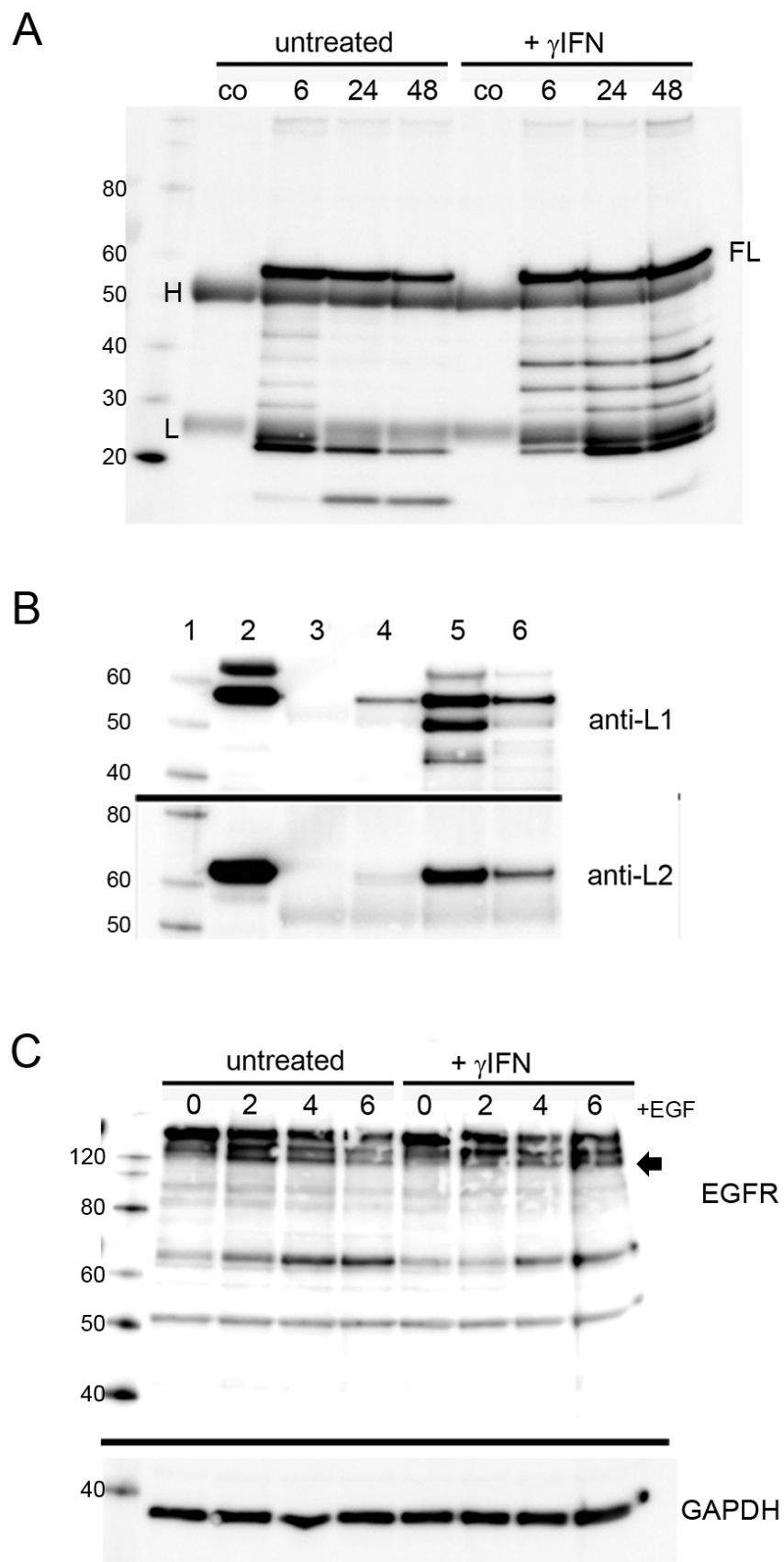
- 766 38. **Ashkar AA, Rosenthal KL.** 2003. Interleukin-15 and natural killer and NKT cells play a critical role
767 in innate protection against genital herpes simplex virus type 2 infection. *J Virol* **77**:10168-
768 10171.
- 769 39. **Schroder K, Hertzog PJ, Ravasi T, Hume DA.** 2004. Interferon-gamma: an overview of signals,
770 mechanisms and functions. *J Leukoc Biol* **75**:163-189.
- 771 40. **Ramana CV, Gil MP, Schreiber RD, Stark GR.** 2002. Stat1-dependent and -independent
772 pathways in IFN-gamma-dependent signaling. *Trends Immunol* **23**:96-101.
- 773 41. **Monath TP, Arroyo J, Levenbook I, Zhang ZX, Catalan J, Draper K, Guirakhoo F.** 2002. Single
774 mutation in the flavivirus envelope protein hinge region increases neurovirulence for mice and
775 monkeys but decreases viscerotropism for monkeys: relevance to development and safety
776 testing of live, attenuated vaccines. *J Virol* **76**:1932-1943.
- 777 42. **Halfter UM, Derbyshire ZE, Vaillancourt RR.** 2005. Interferon-gamma-dependent tyrosine
778 phosphorylation of MEKK4 via Pyk2 is regulated by annexin II and SHP2 in keratinocytes.
779 *Biochem J* **388**:17-28.
- 780 43. **Cerqueira C, Samperio Ventayol P, Vogeley C, Schelhaas M.** 2015. Kallikrein-8 Proteolytically
781 Processes Human Papillomaviruses in the Extracellular Space To Facilitate Entry into Host Cells. *J*
782 *Virol* **89**:7038-7052.
- 783 44. **Bienkowska-Haba M, Williams C, Kim SM, Garcea RL, Sapp M.** 2012. Cyclophilins facilitate
784 dissociation of the human papillomavirus type 16 capsid protein L1 from the L2/DNA complex
785 following virus entry. *J Virol* **86**:9875-9887.
- 786 45. **Barry AO, Mege JL, Ghigo E.** 2011. Hijacked phagosomes and leukocyte activation: an intimate
787 relationship. *J Leukoc Biol* **89**:373-382.
- 788 46. **Montaner LJ, da Silva RP, Sun J, Sutterwala S, Hollinshead M, Vaux D, Gordon S.** 1999. Type 1
789 and type 2 cytokine regulation of macrophage endocytosis: differential activation by IL-4/IL-13
790 as opposed to IFN-gamma or IL-10. *J Immunol* **162**:4606-4613.
- 791 47. **Pei G, Repnik U, Griffiths G, Gutierrez MG.** 2014. Identification of an immune-regulated
792 phagosomal Rab cascade in macrophages. *Journal of cell science* **127**:2071-2082.
- 793 48. **Pei G, Schnettger L, Bronietzki M, Repnik U, Griffiths G, Gutierrez MG.** 2015. Interferon-
794 gamma-inducible Rab20 regulates endosomal morphology and EGFR degradation in
795 macrophages. *Molecular biology of the cell* **26**:3061-3070.
- 796 49. **Arunachalam B, Phan UT, Geuze HJ, Cresswell P.** 2000. Enzymatic reduction of disulfide bonds
797 in lysosomes: characterization of a gamma-interferon-inducible lysosomal thiol reductase (GILT).
798 *Proc Natl Acad Sci U S A* **97**:745-750.
- 799 50. **Phan UT, Arunachalam B, Cresswell P.** 2000. Gamma-interferon-inducible lysosomal thiol
800 reductase (GILT). Maturation, activity, and mechanism of action. *J Biol Chem* **275**:25907-25914.
- 801 51. **Luster AD, Weinshank RL, Feinman R, Ravetch JV.** 1988. Molecular and biochemical
802 characterization of a novel gamma-interferon-inducible protein. *J Biol Chem* **263**:12036-12043.
- 803 52. **Haque MA, Li P, Jackson SK, Zarour HM, Hawes JW, Phan UT, Maric M, Cresswell P, Blum JS.**
804 2002. Absence of gamma-interferon-inducible lysosomal thiol reductase in melanomas disrupts
805 T cell recognition of select immunodominant epitopes. *J Exp Med* **195**:1267-1277.
- 806 53. **Dautry-Varsat A, Ciechanover A, Lodish HF.** 1983. pH and the recycling of transferrin during
807 receptor-mediated endocytosis. *Proc Natl Acad Sci U S A* **80**:2258-2262.
- 808 54. **Hopkins CR, Trowbridge IS.** 1983. Internalization and processing of transferrin and the
809 transferrin receptor in human carcinoma A431 cells. *The Journal of cell biology* **97**:508-521.
- 810 55. **Wiley HS, Herbst JJ, Walsh BJ, Lauffenburger DA, Rosenfeld MG, Gill GN.** 1991. The role of
811 tyrosine kinase activity in endocytosis, compartmentation, and down-regulation of the
812 epidermal growth factor receptor. *J Biol Chem* **266**:11083-11094.

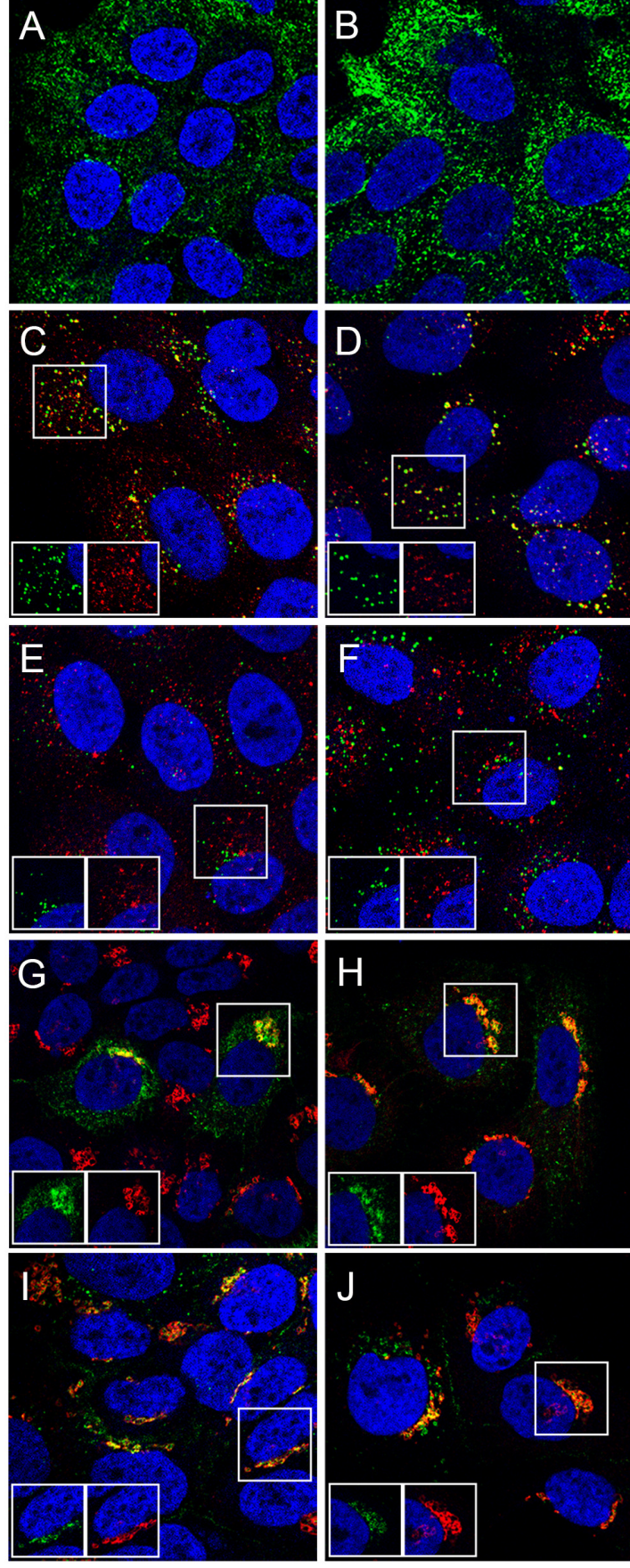
- 813 56. **Chang CP, Lazar CS, Walsh BJ, Komuro M, Collawn JF, Kuhn LA, Tainer JA, Trowbridge IS,**
814 **Farquhar MG, Rosenfeld MG, et al.** 1993. Ligand-induced internalization of the epidermal
815 growth factor receptor is mediated by multiple endocytic codes analogous to the tyrosine motif
816 found in constitutively internalized receptors. *J Biol Chem* **268**:19312-19320.
- 817 57. **French AR, Sudlow GP, Wiley HS, Lauffenburger DA.** 1994. Postendocytic trafficking of
818 epidermal growth factor-receptor complexes is mediated through saturable and specific
819 endosomal interactions. *J Biol Chem* **269**:15749-15755.
- 820 58. **van Deurs B, Holm PK, Sandvig K.** 1996. Inhibition of the vacuolar H(+)-ATPase with bafilomycin
821 reduces delivery of internalized molecules from mature multivesicular endosomes to lysosomes
822 in HEp-2 cells. *Eur J Cell Biol* **69**:343-350.
- 823 59. **Iversen TG, Skretting G, Llorente A, Nicoziani P, van Deurs B, Sandvig K.** 2001. Endosome to
824 Golgi transport of ricin is independent of clathrin and of the Rab9- and Rab11-GTPases.
825 *Molecular biology of the cell* **12**:2099-2107.
- 826 60. **Stechmann B, Bai SK, Gobbo E, Lopez R, Merer G, Pinchard S, Panigai L, Tenza D, Raposo G,**
827 **Beaumelle B, Sauvaire D, Gillet D, Johannes L, Barbier J.** 2010. Inhibition of retrograde
828 transport protects mice from lethal ricin challenge. *Cell* **141**:231-242.
- 829 61. **Hindmarsh PL, Laimins LA.** 2007. Mechanisms regulating expression of the HPV 31 L1 and L2
830 capsid proteins and pseudovirion entry. *Virology* **4**:19.
- 831 62. **Day PM, Thompson CD, Lowy DR, Schiller JT.** 2015. The HPV16 and MusPV1 papillomaviruses
832 initially interact with distinct host components on the basement membrane. *Virology* **481**:79-94.
- 833 63. **Finnen RL, Erickson KD, Chen XS, Garcea RL.** 2003. Interactions between papillomavirus L1 and
834 L2 capsid proteins. *J Virol* **77**:4818-4826.
- 835 64. **Der SD, Zhou A, Williams BR, Silverman RH.** 1998. Identification of genes differentially
836 regulated by interferon alpha, beta, or gamma using oligonucleotide arrays. *Proc Natl Acad Sci U*
837 *S A* **95**:15623-15628.
- 838 65. **Metz P, Dazert E, Ruggieri A, Mazur J, Kaderali L, Kaul A, Zeuge U, Windisch MP, Trippler M,**
839 **Lohmann V, Binder M, Frese M, Bartenschlager R.** 2012. Identification of type I and type II
840 interferon-induced effectors controlling hepatitis C virus replication. *Hepatology* **56**:2082-2093.
- 841 66. **Sadler AJ, Williams BR.** 2008. Interferon-inducible antiviral effectors. *Nat Rev Immunol* **8**:559-
842 568.
- 843 67. **Abend JR, Low JA, Imperiale MJ.** 2007. Inhibitory effect of gamma interferon on BK virus gene
844 expression and replication. *J Virol* **81**:272-279.
- 845 68. **De-Simone FI, Sariyer R, Otalora YL, Yarandi S, Craigie M, Gordon J, Sariyer IK.** 2015. IFN-
846 Gamma Inhibits JC Virus Replication in Glial Cells by Suppressing T-Antigen Expression. *PLoS One*
847 **10**:e0129694.
- 848 69. **Karupiah G, Xie QW, Buller RM, Nathan C, Duarte C, MacMicking JD.** 1993. Inhibition of viral
849 replication by interferon-gamma-induced nitric oxide synthase. *Science* **261**:1445-1448.
- 850 70. **Patterson JB, Thomis DC, Hans SL, Samuel CE.** 1995. Mechanism of interferon action: double-
851 stranded RNA-specific adenosine deaminase from human cells is inducible by alpha and gamma
852 interferons. *Virology* **210**:508-511.
- 853 71. **Lin HY, Yen PM, Davis FB, Davis PJ.** 1997. Protein synthesis-dependent potentiation by
854 thyroxine of antiviral activity of interferon-gamma. *Am J Physiol* **273**:C1225-1232.
- 855 72. **Anderson SL, Carton JM, Lou J, Xing L, Rubin BY.** 1999. Interferon-induced guanylate binding
856 protein-1 (GBP-1) mediates an antiviral effect against vesicular stomatitis virus and
857 encephalomyocarditis virus. *Virology* **256**:8-14.
- 858 73. **Zamanian-Daryoush M, Mogensen TH, DiDonato JA, Williams BR.** 2000. NF-kappaB activation
859 by double-stranded-RNA-activated protein kinase (PKR) is mediated through NF-kappaB-
860 inducing kinase and IkappaB kinase. *Mol Cell Biol* **20**:1278-1290.

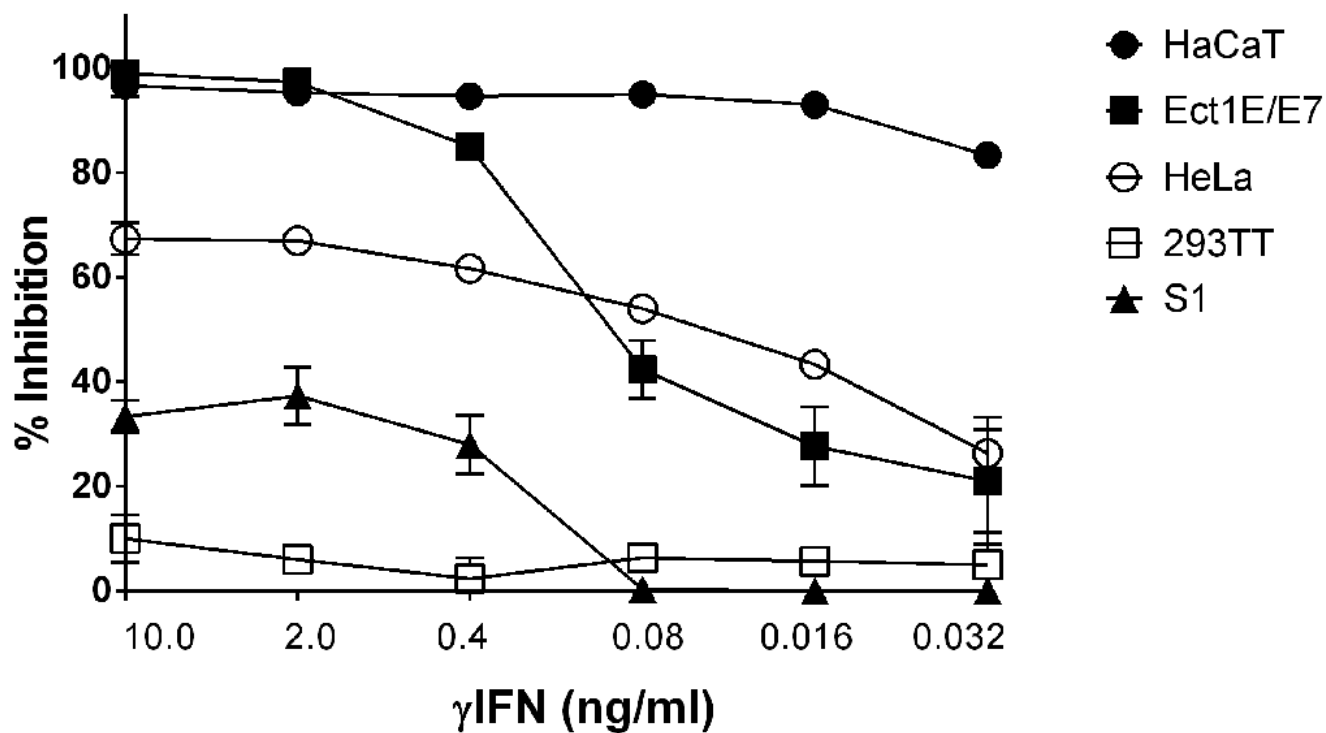
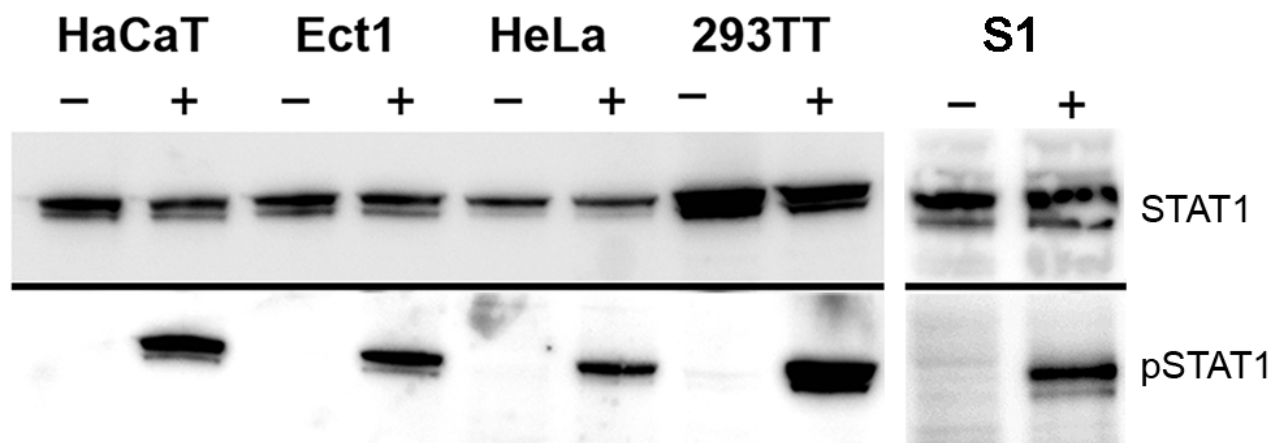
- 861 74. **Burdeinick-Kerr R, Griffin DE.** 2005. Gamma interferon-dependent, noncytolytic clearance of
862 sindbis virus infection from neurons in vitro. *J Virol* **79**:5374-5385.
- 863 75. **Rhein BA, Powers LS, Rogers K, Anantpadma M, Singh BK, Sakurai Y, Bair T, Miller-Hunt C, Sinn
864 P, Davey RA, Monick MM, Maury W.** 2015. Interferon-gamma Inhibits Ebola Virus Infection.
865 *PLoS Pathog* **11**:e1005263.
- 866 76. **Ronco LV, Karpova AY, Vidal M, Howley PM.** 1998. Human papillomavirus 16 E6 oncoprotein
867 binds to interferon regulatory factor-3 and inhibits its transcriptional activity. *Genes Dev*
868 **12**:2061-2072.
- 869 77. **Li S, Labrecque S, Gauzzi MC, Cuddihy AR, Wong AH, Pellegrini S, Matlashewski GJ, Koromilas
870 AE.** 1999. The human papilloma virus (HPV)-18 E6 oncoprotein physically associates with Tyk2
871 and impairs Jak-STAT activation by interferon-alpha. *Oncogene* **18**:5727-5737.
- 872 78. **Park JS, Kim EJ, Kwon HJ, Hwang ES, Namkoong SE, Um SJ.** 2000. Inactivation of interferon
873 regulatory factor-1 tumor suppressor protein by HPV E7 oncoprotein. Implication for the E7-
874 mediated immune evasion mechanism in cervical carcinogenesis. *J Biol Chem* **275**:6764-6769.
- 875 79. **Barnard P, McMillan NA.** 1999. The human papillomavirus E7 oncoprotein abrogates signaling
876 mediated by interferon-alpha. *Virology* **259**:305-313.
- 877 80. **Chang YE, Pena L, Sen GC, Park JK, Laimins LA.** 2002. Long-term effect of interferon on
878 keratinocytes that maintain human papillomavirus type 31. *J Virol* **76**:8864-8874.
- 879 81. **Herdman MT, Pett MR, Roberts I, Alazawi WO, Teschendorff AE, Zhang XY, Stanley MA,
880 Coleman N.** 2006. Interferon-beta treatment of cervical keratinocytes naturally infected with
881 human papillomavirus 16 episomes promotes rapid reduction in episome numbers and
882 emergence of latent integrants. *Carcinogenesis* **27**:2341-2353.
- 883 82. **Maher SG, Sheikh F, Scarzello AJ, Romero-Weaver AL, Baker DP, Donnelly RP, Gamero AM.**
884 2008. IFNalpha and IFNlambda differ in their antiproliferative effects and duration of JAK/STAT
885 signaling activity. *Cancer Biol Ther* **7**:1109-1115.
- 886 83. **Feeley EM, Sims JS, John SP, Chin CR, Pertel T, Chen LM, Gaiha GD, Ryan BJ, Donis RO, Elledge
887 SJ, Brass AL.** 2011. IFITM3 inhibits influenza A virus infection by preventing cytosolic entry. *PLoS*
888 *Pathog* **7**:e1002337.
- 889 84. **Via LE, Fratti RA, McFalone M, Pagan-Ramos E, Deretic D, Deretic V.** 1998. Effects of cytokines
890 on mycobacterial phagosome maturation. *Journal of cell science* **111 (Pt 7)**:897-905.
- 891 85. **Trost M, English L, Lemieux S, Courcelles M, Desjardins M, Thibault P.** 2009. The phagosomal
892 proteome in interferon-gamma-activated macrophages. *Immunity* **30**:143-154.
- 893 86. **Yates RM, Hermetter A, Taylor GA, Russell DG.** 2007. Macrophage activation downregulates the
894 degradative capacity of the phagosome. *Traffic* **8**:241-250.
- 895



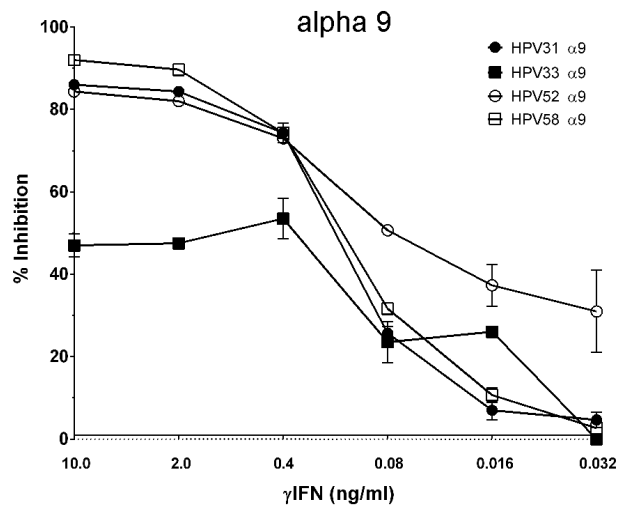




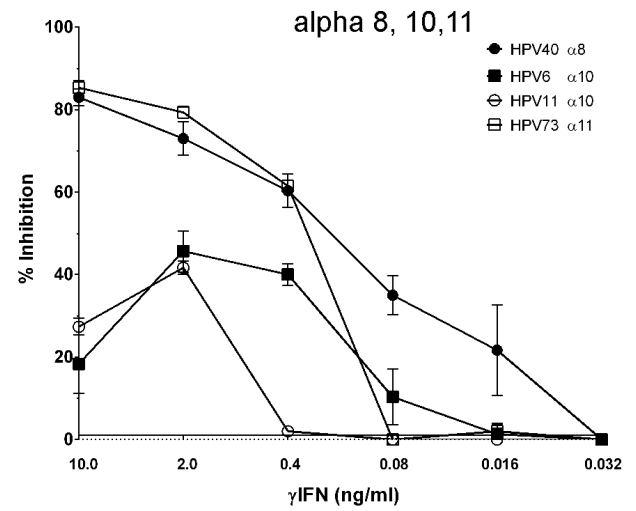


A**B**

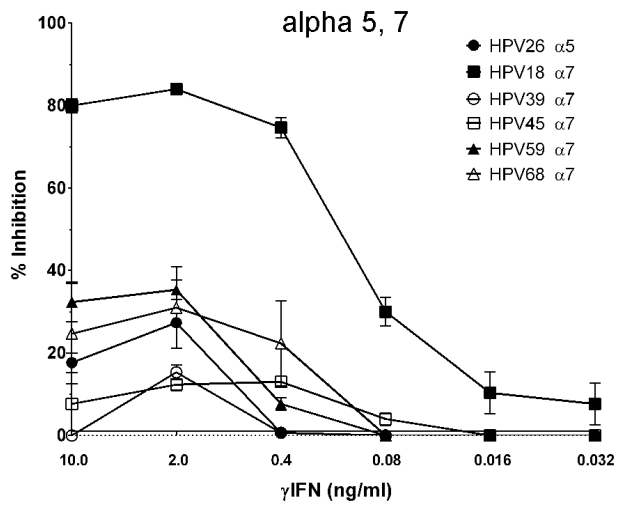
A



B



C



D

